Sudan University of Science and Technology

College of Graduate Studies

دراسة تعزيز التباين في انسجة الدماغ الطبيعية والمريضة في صور الرنين المغناطيسي

Study of Contrast-Enhancement in Normal and Pathological Brain Tissue in Magnetic Resonance Image

A Thesis Submitted For Partial Fulfillment For The Requirements Of (M.SC)

Degree In Medical Physics

by:

Omsalama Omer Hassan Ali

Supervisor:

Dr. Hussein Ahmed Hassan

2017

بِسْمِ اللَّهِ الرَّحْمَنِ الرَّحِيمِ

الرَّحْمَنُ (1) عَلَّمَ الْقُرْآنَ (2) خَلَقَ الْإِنْسَانَ (3) عَلَّمَهُ الْبَيَانَ (4) الشَّمْسُ وَالْقَمَرُ بِحُسْبَانٍ (5) وَالنَّجْمُ وَالشَّجَرُ يَسْجُدَانِ (6) وَالسَّمَاءَ رَفَعَهَا وَوَضَعَ الْمِيزَانَ (7) أَلَّا تَطْغَوْا فِي الْمِيزَانِ (8) وَأَقِيمُوا الْوَزْنَ بِالْقِسْطِ وَلَا تُخْسِرُوا الْمِيزَانَ (9) وَالْأَرْضَ وَضَعَهَا لِلْأَنَامِ (10) فِيهَا فَاكِهَةٌ وَالنَّخْلُ ذَاتُ الْأَكْمَامِ (11) وَالْحَبُّ ذُو الْعَصْفِ وَالرَّيْحَانُ (12) فَبِأَيِّ آلَاءِ رَبِّكُمَا تُكَذِّبَانِ (13) خَلَقَ الْإِنْسَانَ مِنْ صَلْصَالٍ كَالْفَخَّارِ (14) وَخَلَقَ الْجَانَّ مِنْ مَارِجٍ مِنْ نَارٍ (15) فَبِأَيِّ آلَاءِ رَبِّكُمَا تُكَذِّبَانِ (16).

(الرحمن 1-16)

Acknowledgment

Many thanks to Allah Almighty who helped me to write this thesis.

My sincere thanks to Dr. Hussein Ahmed Hassan for his great help, guidance, encouragement and valuable advices.

I am grateful to Austaz. Murtada Mohammed Ibrahim and to those colleagues in Antalya Medical Center who helped me in collecting the data and for their continuous attention and valuable advices.

Finally my thanks to my family and my friends who always encourage and support me.

Dedication

This thesis is dedicated to:

The spirit of my father

The spirit of my husband

My Mother

My brother and sisters

Contents

List of Tables

List of figures

List of abbreviation

MRI	Magnetic resonance imaging
NMR	nuclear magnetic resonance
CT	Computer Tomography
Si	signal intensity
WM	Cerebral White matter
GM	Cerebral Gray matter
CSF	Cerebrospinal fluid
RF	Radio-frequency
CE	contrast-enhanced
Gd-DTPA	gadolinium-diethylenetriaminepenta-acetic acid
MTC	Magnetization transfer contrast
SNR	signal to noise ratio
MT	magnetization transfer
TE	The echo time
TR	The repetition time
TI	The time of inversion
T1 W1	Time weighted image
T2 W2	Time weighted image
SE	Spin Echo
FOV	Field Of View
FLAIR	Fluid Attenuation Inverse Recovery
PSNR	Signal to Noise Ratio
Sig.	significant value
Std. Deviation	Standard Deviation
(2-tailed)	Test for inequality of tow means
Std. Error Mean	Standard Error of Mean
T	Student’s t-test statistic
Chi-square test	Pearson Chi-square test for association
Df	Degree of freedom
QC	Quality Control

Abstract

The aim of this study was to determine if a contrast agent provides additional information for characterization of brain lesion and normal tissue.

The advantages of magnetic resonance imaging (MRI) over other diagnostic imaging modalities are its higher spatial resolution and its better discrimination of soft tissue.

This study of brain diseases relied on quantitative measures obtained from MR scans that are segmented into the three common tissue types present in the human brain: cerebral gray matter (GM), cerebral white matter (WM), and cerebral spinal fluid (CSF).
The study was carried out in Antalya Medical Center during the period from July to October and included 63 brain lesion patients.

The performance of contrast agent was evaluated by measuring signal intensity and comparing the diagnostic accuracy of MRI image with contrast and without contrast.

The results indicate that the same effect of Contrast on Lesion tissue and normal tissue for all ages and for both males and females and the diagnosis doesn't dependent on age or gender.

The results showed the effectiveness of the contras agent and the achieved improvement in image quality. As the contrast agent improves the detection of brain lesion according to the type of lesion, this was clearly shown by the results.

Also the results indicate that the ability of contrast-enhanced MRI to identify additional information for characterization of Pathological Brain Tissue and Enhanced the normal tissue according to the type of tissue.

المـلخـص

هدف هذه الدراسة تحديد ما اذا كان عامل التباين يضيف معلومات لتشخيص امراض الدماغ ., تم تقييم عامل التباين بقياس شدة الاشاره و مقارنة دقة التشخيص لصورة الرنين المغناطيسى قبل وبعد استخدام عامل التباين.

من مميزات استخدام التصوير الطبى بالرنين المغناطيسى على اشكال التصوير التشخيصى الاخرى ان الرنين المغناطيسى يوضح تفاصيل الصوره بدقه عاليه للأنسجه اللينه.

هذه الدراسه لامراض الراس تعتمد على القياسات الكميه الماخوذه من المسح بالرنين المغنطيسي لانواع الانسجة الثلاثة الموجودة في الدماغ البشري, مادة الدماغ الرماديه ومادة الدماغ البيضاء,والسائل الدماغي الشوكي.

اجريت هذه الدراسة في مركز انطاليا الطبي ,اشترك في هذه الدراسة63 مريض دماغي.

اظهرت النتائج فعالية عامل التباين في تحسين جودة الصوره وان عامل التباين يحسن اكتشاف امراض الدماغ بشكل ملحوظ لكن تحسينه متفاوت لانواع اصابات الدماغ.

ايضا تشير النتائج إلى قدرة عامل التباين على تعزيز التصوير بالرنين المغناطيسي لتحديد معلومات إضافية لتوصيف الأنسجة الدماغية المريضه و تعزيز الأنسجة الدماغية الطبيعية وفقا لنوع النسيج.

Chapter One

Chapter one

1-1. Introduction

Magnetic resonance imaging (MRI) is a spectroscopic imaging technique used in medical settings to produce images of the inside of the human body. MRI is based on the principles of nuclear magnetic resonance (NMR), which is a spectroscopic technique used to obtain microscopic chemical and physical data about molecules. (www.slideworld.org,11-5-2017,3:00pm)

The magnetic resonance imaging is accomplished through the absorption and emission of energy of the radio frequency (RF) range of the electromagnetic spectrum.(www.slideworld.org,11-5-2017,3:00pm)

Magnetic resonance imaging (MRI) is a noninvasive medical test that physicians use to diagnose and treat medical conditions.MRI uses a powerful magnetic field, radio frequency pulses and a computer to produce detailed pictures of organs, soft tissues, bone and virtually all other internal body structures. MRI does not use ionizing radiation (x-rays). (www.radiologyinfo.org, 11-5-2017, 3:08pm)

Detailed MR images allow physicians to evaluate various parts of the body and determine the presence of certain diseases. The images can then be examined on a computer monitor, transmitted electronically, printed or copied to a CD. (www.radiologyinfo.org, 11-5-2017, 3:08pm)

MRI is a rapidly changing and growing image modality. The high contrast sensitivity to soft tissue differences and the inherent safety to the patient resulting from the use of nonionizing radiation have been key reasons why MRI has supplanted many CT and projection radiography methods. With continuous improvements in image quality, acquisition methods, and equipment design, MRI is the modality of choice to examine anatomic and physiologic properties of the patient. (JERROLD,etal,2002)

The differentiation between normal and diseased tissue by means of magnetic resonance (MR) imaging relies on their distinctive signal intensity (SI) which depends, among other factors, on intrinsic properties of tissue (T1 and T2 relaxation times). However, the relaxation times of

normal and abnormal tissues frequently over-lap. As a consequence, the ability of plain MR imaging to detect and to characterize abnormal tissue may be compromised. This shortcoming is, however, overcome by applying specialized pulse sequences, or instead by using MR contrast agents, substances which change the tissue relaxation times and can, therefore, be administered in order to manipulate their signal intensity. (Luis, etal, 2011)

In clinical practice, contrast media with paramagnetic or super paramagnetic properties are used to shorten the T1 and T2 relaxation times (Luis,etal,2011)

MRI contrast agents are a group of contrast media used to improve the visibility of internal body structures in Magnetic resonance imaging (MRI). The most commonly used compounds for contrast enhancement are gadolinium-based. Such MRI contrast agents shorten the relaxation times of nuclei within body tissues following oral or intravenous administration. (www.wikipedia.org, 11-5-2017,)

A contrast agent usually shortens, but in some instances increases the value of T1 of nearby water protons thereby altering the contrast in the image. (www.theydiffer.com)

MRI is particularly useful for the imaging of soft tissues. Therefore, MRI allows for high-quality imaging of the brain with good anatomic detail and offers more sensitivity and specificity than other imaging modalities for many types of neurological conditions. MRI can be useful in evaluation of the Ischemia/infarct, Vascular anomalies, Hemorrhage, Infection, Tumors and masses, Trauma and diffuse axonal ,njuries,Neurodegenerative disorders and dementias, Inflammatory conditions, Congenital abnormalities, Seizures, Headaches, Cranial neuropathies ,Fetal brain .(www.emedicine.medscape.com)

1-2.Problems of study:

Sometimes the MRI image is not accurate which can decrease the image quality and can lead to miss diagnosis and then when administrate MRI contrast media it will be lead to differentiate between the normal and disease tissue by enhancing the pathological tissue.

1-3. Objectives:

1-3-1. General Objective:

To study contrast-enhancement in normal and pathological brain tissue.

1-3-2.Specific Objectives:

- To compare between the diagnostic accuracy of MRI with Contrast and MRI without Contrast

-To identify image quality in MRI Brian T1 weighted imaging for brain lesion with Contrast vs. without Contrast.

To determine if a contrast agent provides additional information for characterization of brain lesion and normal tissue.

1-4. Overview of the study:

This study consists of five chapters:

chapter one includes introduction, problem statement and Objectives , chapter two deals with theoretical background including literature review and Previous Studies, chapter three deals with materials and methods while chapter four deals with the analysis results and five shows discussion ,conclusion and recommendation.

Chapter Two

Chapter two

Literature review and theoretical

For thirty years now, magnetic resonance imaging (MRI) has been routinely used in hospitals worldwide as a non-invasive and non-ionizing imaging technique. Based on the nuclear magnetic resonance (NMR) phenomenon observed in 1946 for protons by Bloch and Purcell, MRI was developed only in 1973 by Lauterbur and Mansfield, notably because it required some important progress in technology and informatics. For their contributions to the development of MRI, Paul Lauterbur and Peter Mansfield received the Nobel Prize in medicine in 2003. The evolution of the initial method has been vertiginous: the time needed to acquire an image has been divided by 100, the resolution is now below the millimeter, and the development of new imaging sequences is a science in itself. There are numerous MRI applications in the clinical field, including the detection of tumors, functional imaging of the brain, angiography, brain fiber analysis, parallel imaging, etc. MRI has also found industrial applications, in the food industry for example. (Gossuin, etal, 2010)

2-1. MRI physics:

MRI is based on quantum mechanics, uses advanced technology for creating strong magnetic field gradients, for radiofrequency excitation and detection. The image formation is based on mathematical transformations executed by efficient informatics systems. This wide variety of disciplines involved in MRI, combined with the mainly biological applications, makes it sometimes difficult to understand. The aim of this short—and incomplete—introduction to MRI is to give a basic description of the physical principles of this imaging technique. (Gossuin, etal, 2010)

The standard unit of measurement of the magnetic field strength is Tesla (T). One T is equal to 10,000 Gauss (G). The earth's magnetic field strength at the surface is 0.5 G to 2.0 G. (Ontario Health Technology Assessment Series 2003;3).

2-1-1. Nuclear magnetic resonance

2-1-1-1. Magnetic properties of the atomic nucleus

Each nucleus possesses a kinetic momentum J, related to its spin I by

$$\vec{J} = \hbar \vec{I}. \qquad (2\text{-}1)$$

The measurable values of the projection of the kinetic momentum in a random direction, arbitrarily taken as the z-axis, are thus

$$J_z = \hbar I, \hbar(I-1), \hbar(I-2), ..., -\hbar(I-2), -\hbar(I-1), -\hbar I.$$

One can assign a magnetic moment to the nucleus thanks to the relation:

$$\vec{\mu} = \gamma \vec{J}. \qquad (2\text{-}2)$$

where γ is the gyro magnetic ratio of the nucleus

$\gamma = g_n \beta/\hbar$, g_n is the Landé factor of the studied nucleus and

$\beta = e\hbar/2m_p$ is the nuclear Bohr magneton.

The projection of the nucleus magnetic moment in the z-direction is thus also quantified,

$$\mu_z = \gamma J_z.$$

Only the nuclei having a non-null magnetic moment—thus a non-null spin—are observable by NMR. The resulting spin of a nucleus depends on the number of protons and neutrons it contains. It is non-null if the number of protons is odd or if it is even with an odd number of neutrons. The NMR behavior may thus be different for isotopes of the same element. The NMR sensitivity of a given isotope takes into account its natural abundance and the amplitude of the NMR signal it

produces, depending on its gyro magnetic ratio.
(Gossuin, etal, 2010)

2-1-2. Protons under a magnetic field

2-1-2-1. Quantum approach

For a proton, the possible values of μz are

$$\mu_z = \pm\gamma\hbar/2 \text{ since } I = 1/2$$

In the absence of a magnetic field, there is degeneracy because the energies corresponding to these two values of μz are equal. However, if a magnetic field $\vec{B}_0$ is applied along the *z*-direction, the energy levels will split because of the Zeeman coupling between the nuclear magnetic moment and the magnetic field (figure 1). This can be described by the following Hamiltonian:

$$H = -\vec{\mu} \cdot \vec{B}_0. \qquad (2\text{ -}3)$$

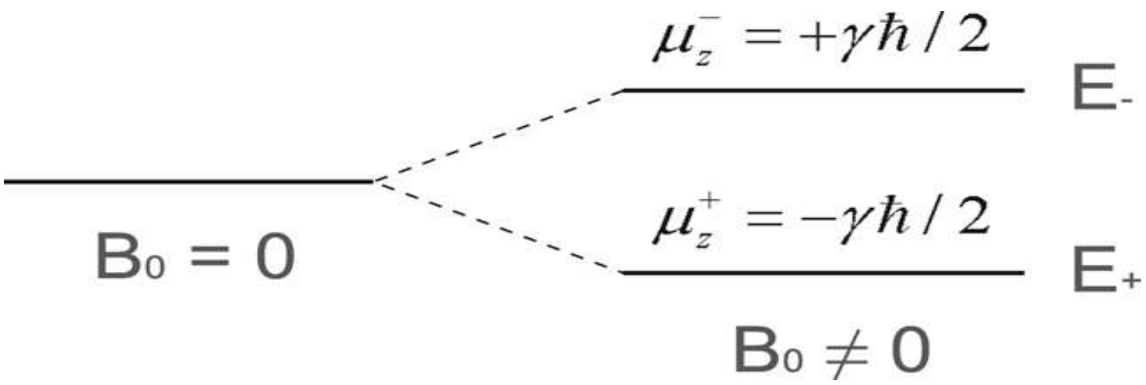

(**Figure 2-1**. Zeeman splitting of the proton energy levels)

The two Eigen values *E*+ and *E*− of this Hamiltonian correspond to the energies of the protons with μz, respectively, aligned and anti-aligned with the magnetic field:

$$E_+ = -\gamma\hbar B_0/2 \quad \text{and} \quad E_- = +\gamma\hbar B_0/2. \qquad (2\text{-}4)$$

The energy difference between the two levels is simply given by

$$\Delta E = \hbar \gamma B_0 = \hbar \omega_0 \qquad (2\text{-}5)$$

Where $\omega_o = \gamma B_o$

is called the Larmor angular frequency. The excitation of a proton from the *E*+ level to the *E*− level requires a photon with the right energy, Δ*E*, and therefore the right frequency, called the Larmor frequency:

$$\nu_0 = \gamma B_0 / 2\pi \qquad (2\text{-}6)$$

For a population of *N* protons at a constant temperature, the distribution of the two energy levels will follow a Boltzmann statistic. If *N*+ and *N*− are, respectively, the number of protons with *E*+ and *E*−, one obtains

$$\frac{N_+}{N_-} = e^{\hbar\omega_0/kT}, \qquad (2\text{-}7)$$

where *T* is the absolute temperature and *k* the Boltzmann constant. For usual magnetic fields, *N*+ *N*−, there are a few more protons with μz aligned than anti-aligned with $\vec{B}_0$. The system of protons behaves like a paramagnet: under the application of a magnetic field, it acquires a magnetic moment with the same direction as the field. It can be calculated using a first order development equation (2-7):

$$\mu_0 = N_+\mu_z^+ + N_-\mu_z^- = N\frac{(\gamma\hbar)^2}{4kT}B_0 \qquad (2\text{-}8)$$

For example, one can calculate the magnetic moment of protons of the human body when they are placed inside an MRI scanner using a magnetic field of 3 T. One obtains for a human of 80 kg whose body contains 70% water by weight, μ0 = 5 × 10−4 A m2. This magnetic moment is of the same order as the 'electronic' diamagnetic moment of 20 g of water in the same magnetic field. This explains why the 'static' magnetic properties of nuclei are always overwhelmed by the

electronic properties of the atoms they belong to. It is thus impossible to directly measure the static equilibrium magnetic moment of a proton population.

2-1-2-2. Classical approach

A classical description of the behavior of proton magnetic moments in the presence of a magnetic field can be quite useful for understanding MRI acquisition sequences. In this case, the protons have a classical magnetic moment that is related to their kinetic momentum through

$$\vec{\mu} = \frac{e}{2m}\vec{J} \qquad (2\text{-}9)$$

If we take $\gamma = e/2m$, this equation is similar to (2-2). In a static magnetic field $\vec{B}_0$, a torque

$$\vec{\tau} = \vec{\mu} \times \vec{B}_0$$

appears that will modify the kinetic momentum according to the classical relation:

$$\vec{\tau} = \frac{d\vec{J}}{dt} \qquad (2\text{ -}10)$$

The evolution of the magnetic moment is thus given by

$$\frac{d\vec{\mu}}{dt} = \gamma\vec{\mu} \times \vec{B}_0 \qquad (2\text{-}11)$$

One can show that (2-11) describes the precession of the magnetic moment around $\vec{B}_0$ at the Larmor frequency

$$\nu_0 = \gamma B_0/2\pi$$

The rotating reference frame (x', y', z) is defined as the reference frame turning around the z-direction at the Larmor frequency, with, respectively, x and x', and y and y' axes coinciding when $t = 0$. That frame is especially convenient for describing the dynamics of the magnetic moments.

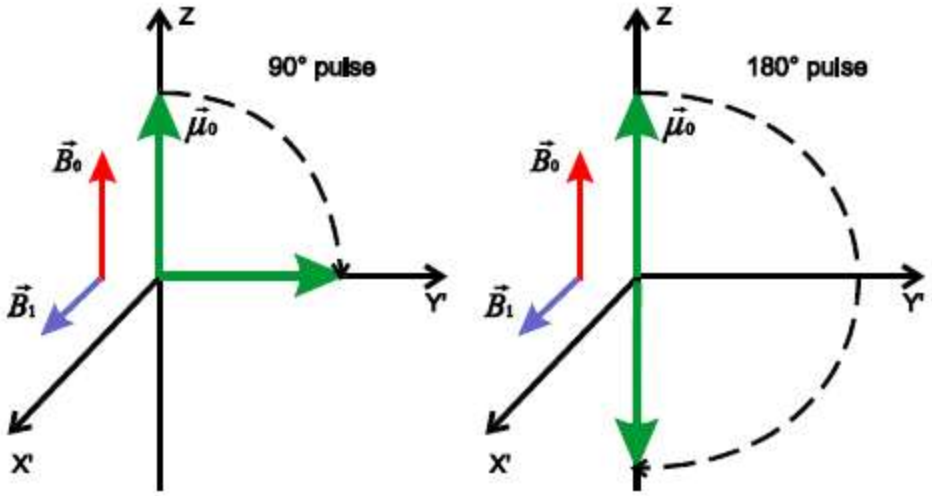

Figure 2-2 . Illustration of 90° and 180° radiofrequency pulses in the rotating frame.

2-1-3. Excitation of the System by a Radiofrequency Field:

To put the system of protons out of equilibrium, we must irradiate the protons with photons having the appropriate frequency

$$\nu_0 = \gamma B_0/2\pi$$

For example, if the static magnetic field is 1 T, the corresponding frequency is 42.6 MHz, corresponding to the radiofrequency domain.

From the quantum point of view, this will cause transitions between the Zeeman energy levels, which will perturb their equilibrium populations.

From a classical point of view, we have to use a magnetic field oscillating at ν0 frequency and perpendicular to $\vec{B}_0$, in the *x*-direction for example. For the rest of the discussion, such a field can be seen as a field $\vec{B}_1(t)$, rotating around the *z*-axis at the Larmor frequency, like the proton magnetic moments1. When $\vec{B}_1(t)$ is applied, equation (2-11) becomes

$$\frac{d\vec{\mu}}{dt} = \gamma\vec{\mu} \times (\vec{B}_0 + \vec{B}_1) \qquad (2\text{-}12)$$

In a frame rotating at the pulsation ω0 following the magnetic moments and the rotating field $\vec{B}_1(t)$, equation (2-12) is modified:

$$\left(\frac{d\vec{\mu}}{dt}\right)_{rot} = \left(\frac{d\vec{\mu}}{dt}\right) + \omega_0 \vec{1}_Z \times \vec{\mu}$$
$$= \gamma \vec{\mu} \times \left(\vec{B}_0 + \vec{B}_1 - \frac{\omega_0}{\gamma}\vec{1}_Z\right) \quad (2\text{ -}13)$$

$\vec{B}_0 = B_0 \vec{1}_Z$ and in the rotating frame, $\vec{B}_1 = B_1 \vec{1}_{X'}$ AS $\omega_0 = \gamma B_0$

relation (13) simplifies to

$$\left(\frac{d\vec{\mu}}{dt}\right)_{rot} = \gamma \vec{\mu} \times B_1 \vec{1}_{X'} \quad (2\text{-}14)$$

This equation is very similar to relation (2-11). When an oscillating magnetic field with the Larmor frequency is applied, the resulting magnetic moment of the proton population rotates around the $\vec{B}_1$ direction in the rotating frame. $\vec{B}_1$ is only efficient if it rotates together with the proton magnetic moment at the Larmor frequency. This is thus a resonance phenomenon. The angular frequency of the rotation of $\vec{\mu}$ around $\vec{B}_1$ in the rotating frame is by analogy $\omega_1 = \gamma B_1$. So the flip angle of the magnetic moment is given by

$$\alpha = \omega_1 t = \gamma B_1 t \quad (2\text{-}15)$$

By varying the duration *t* of application of the *B*1 field (or in some cases by varying its amplitude), one can choose to rotate the resulting magnetic moment of the protons with different angles. The most used flip angles are 90° and 180°; one then speaks of 90° and 180° pulses, respectively (figure 8).

After a radiofrequency pulse tuned at the Larmor frequency, the proton system is out of equilibrium—it will return to equilibrium through transitions between the Zeeman energy levels.

This could not be achieved by spontaneous transitions: their probability is negligible. In fact, the return to equilibrium is caused by time-modulated interactions of the protons with their environment, in a process called relaxation.(Gossuin,etal, 2010)

2-1-4.Return To Equilibrium-T1 Relaxation:

The loss of transverse magnetization (T2 decay) occurs relatively quickly, whereas the return of the excited magnetization to equilibrium (maximum longitudinal magnetization) takes a longer time. Individual excited spins must release their energy to the local tissue (the lattice). Spin-lattice relaxation is a term given for the exponential regrowth of M" and it depends on the characteristics of the spin interaction with the lattice (the molecular arrangement and structure). The T_1 relaxation constant is the time needed to recover 63% of the longitudinal magnetization, M" after a 90-degree pulse (when μ_z = 0). The recovery of μ_z versus time after the 90-degree RF pulse is expressed mathematically as follows:

$$\frac{d\mu_Z(t)}{dt} = -\frac{[\mu_Z(t) - \mu_0]}{T_1} \qquad (2\text{-}16)$$

This leads to an exponential evolution of μz:

$$\mu_Z(t) = \mu_0[1 - 2e^{-t/T_1}] \quad \text{after a } 180^\circ \text{ pulse.} \quad (2\text{ -}17)$$

The return to equilibrium of μz is called the longitudinal relaxation, because it concerns the z-component of the magnetic moment. The time constant T1 is the longitudinal relaxation time.

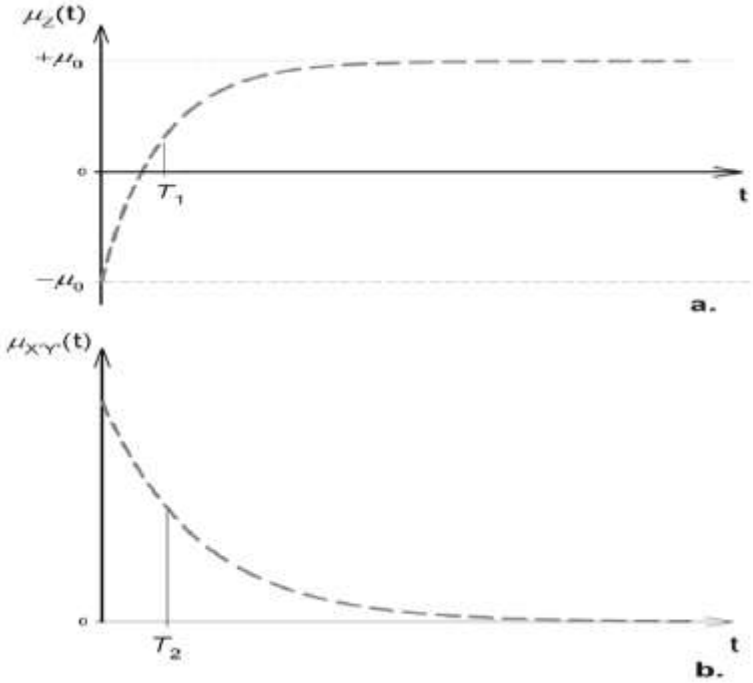

Figure 2-3. Illustration of the return to equilibrium of

(a) μ_z after a 180◦ radiofrequency pulse and (b) $\mu_{x'y'}$ after a 90◦ pulse.

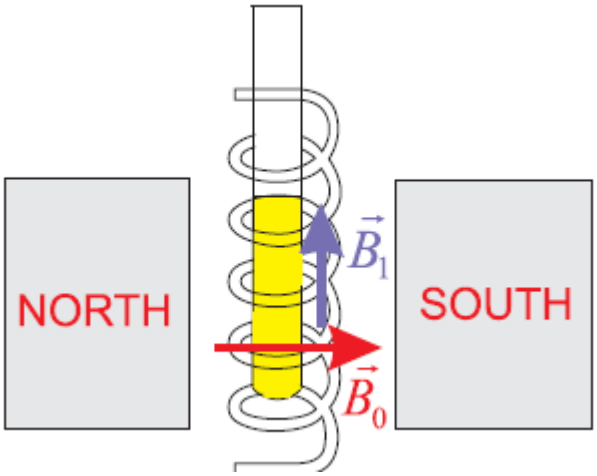

Figure 2-4. Basic NMR experimental setup, with the permanent magnet and the excitation-detection coil.

2.2. MRI Equipment:

Main Magnet (B0), Magnet Shielding, Chiller, RF Transmitter (B1), RF Shield (Faraday's Cage), Gradient Coils (Gx, Gy, Gz), Shim Coils, RF Patient Coils Computer.

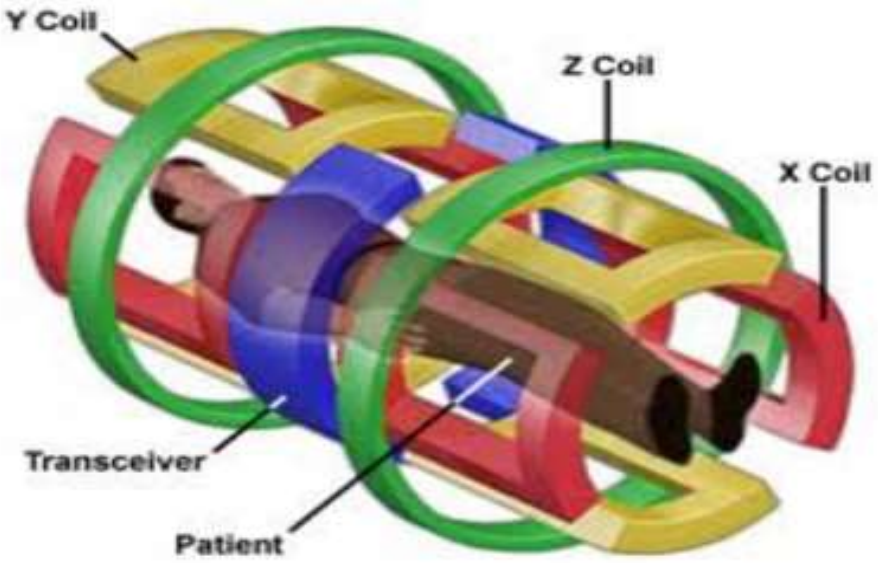

Figure 2-5.a MRI Scanner Gradient Magnets

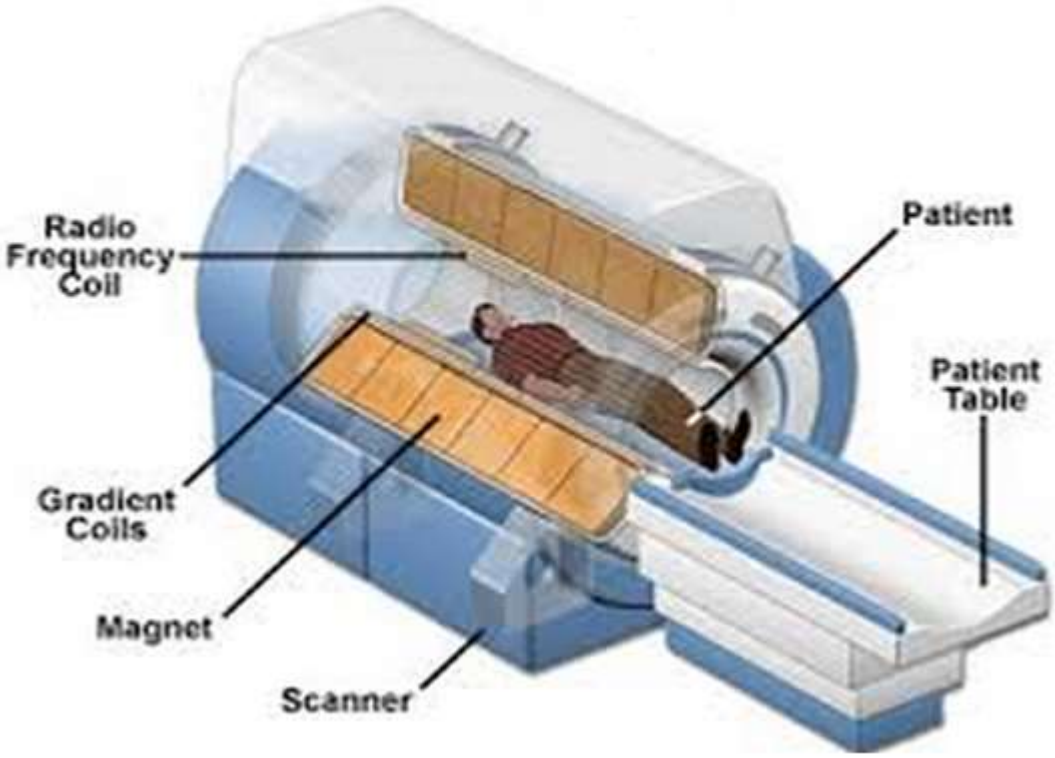

Figure 2-5.b. MRI Scanner Cutaway

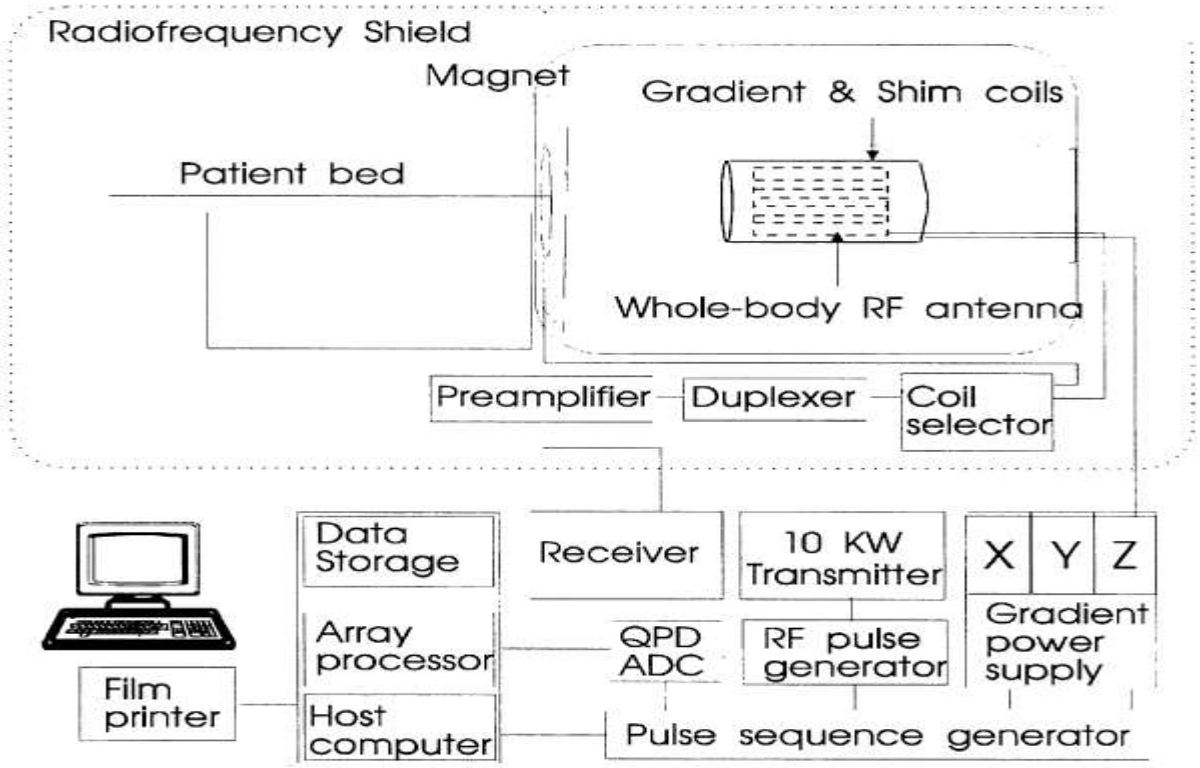

Figure 2.6. The basic components of an MR imager.

2-2-1.Main Magnet (B0):

Three common types:-

-Permanent Magnets (up to 0.4T)

-Resistive and Electromagnets (up to 0.6T)

-Superconducting Magnets (0.5T and higher)

2-2-1-1.Permanent Magnets:

-Are magnets whose magnetic field originates from permanently ferromagnetic materials to generate a magnetic field between the two poles of the magnet.

-There is no requirement for additional electrical power or cooling.

-The iron-core structure of the magnet leads to limited fringe field and limited missile effect.

-Permanent magnets are usually limited to maximum field strengths of 0.4 T due to weight and size considerations.

-The main disadvantages of a permanent magnet are the cost of the magnet and supporting structures, and the varying changes in the magnetic field.

-Field homogeneity can be an on-going problem in permanent magnets.

Figure 2-7 MRI Machine - Permanent Magnets

2-2-1-2.Resistive Magnets:

-Are magnets that utilize the principles of electromagnetism to generate the magnetic field

-Typically large current values and significant cooling of the magnet coils are required

-The resistive magnet does not require cryogens, but needs a constant power supply to maintain a homogenous magnetic field, and can be quite expensive to maintain

-Resistive magnets fall into two general categories -iron-core and air-core

-Iron-core electromagnets provide the advantages of a vertically oriented magnetic field, and a limited fringe field with little, if any, missile effects due to the closed iron-flux return path

-Air-core electromagnets exhibit horizontally oriented fields, which have large fringe fields (unless magnetically shielded) and are prone to missile effects

-Resistive magnets are typically limited to maximum field strengths of approximately 0.6T

Figure 2-8. MRI Machine- Resistive Magnets

2-2-1-3.Superconducting Magnets:-

Superconducting magnets are electromagnets that are partially built from superconducting materials and therefore reach much higher magnetic field Intensity.

- The coil windings of superconducting magnets are made of wires of a type2

superconductor (such as niobium - titanium (NbTi) alloy).

- These coils have no resistance when operated at temperatures near absolute zero

(-273.15°C, - 459°F, 0 K).

-Liquid helium (4.2 K) is commonly used as a coolant.

-Sometimes a second cryogen liquid nitrogen is additionally used as an intermediate thermal shield to reduce the boil-off rate of liquid helium.

-Superconducting magnets typically exhibit field strengths of greater than 0.5 T, operate clinically up to 3 T, and have a horizontal field orientation, which makes them prone to missile effects without significant magnetic shielding.

-High field magnets used in Chemistry have vertical field orientation.

Figure 2-9. MRI Machine -Superconducting Magnets

2-2-1-4.Cryogens:-

Cryogens are cooling agents, typically liquid helium or liquid nitrogen that are used to reduce the temperature of the magnet windings in a superconducting magnet.

All cryogenic liquids are gases at normal temperatures and pressures.

Different cryogens become liquids under different conditions of temperature and pressure.

All have two properties in common, They are extremely cold and Small amounts of liquid can expand into very large volumes of gas, The boiling points of cryogens are commonly below -150°C(-238°F) Transported in Dewar cylinders.

Figure 2-10. Cryogens

2-2-2.Magnet Shielding:-

The goal of magnetic shielding is to protect the environment from the MRI magnetic field Active and Passive shielding Active magnetic shielding uses secondary shielding coils to produce a magnetic field that cancels the field from primary coils in regions where it is not desired These coils may be inside the magnet cryostat Active shielding can be applied to the main magnet or to the gradient magnetic field.

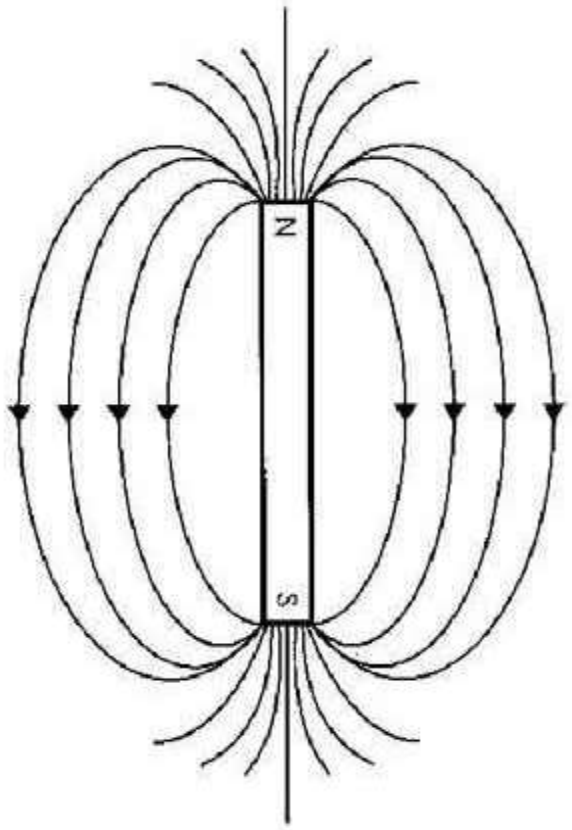

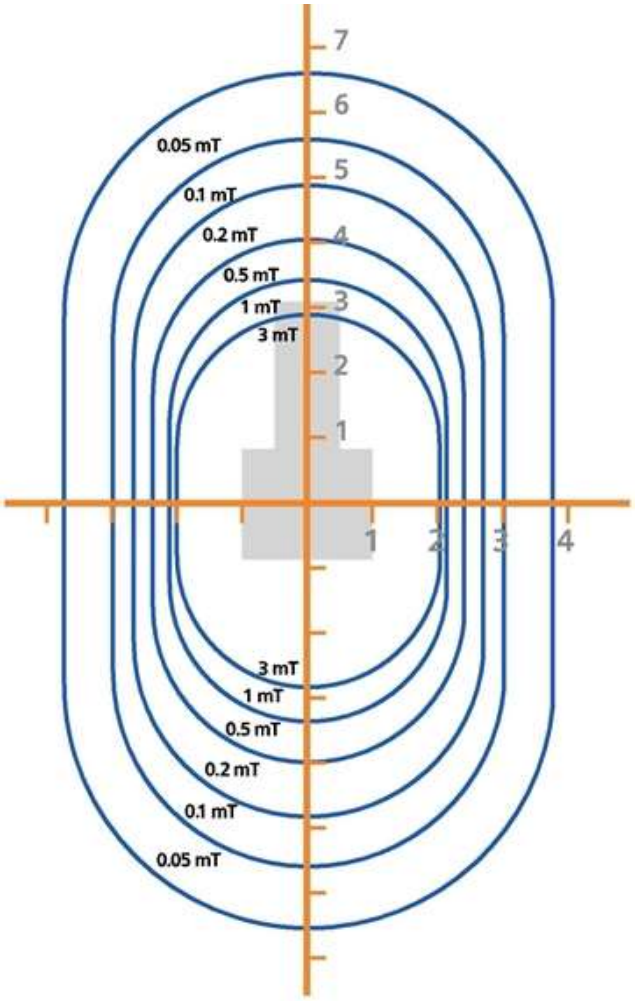

Figure 2-11.a MRI magnetic field

Figure 2-11.b MRI Magnet Shielding

2-2-3.MRI Chiller:-

Chiller is a refrigeration unit that supplies cold water to cool MRI components Chillers are essential for superconducting magnets to reduce the boil-off of Helium and/or Nitrogen.

Depending on the system configuration chillers are used to cool shield coolers, shim coils and sometimes the air conditioning.

Figure 2-12. MRI Chiller

2-2-4.RF Body Coil:-

The body coil is installed in the magnet and functions both as transmit than also as a receiver coil (transceiver).

This coil has a large measurement field, but does not have the high SNR of special coils When specific receiver only coils are used (surface coils), the body coil serves as the transmit coil Modern MRI scanners have RF body coils with multi -transmit features to avoid B1inhomogeneity artifacts.

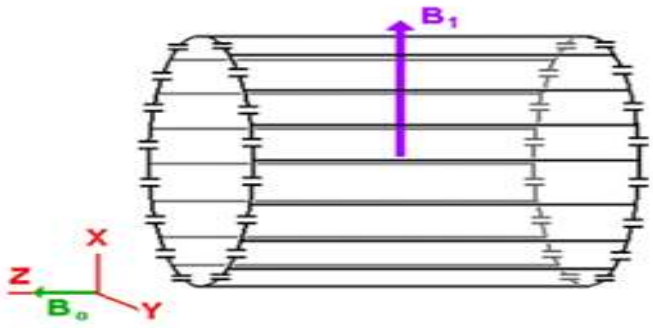

Figure 2-13.Bird Cage Coil (Victor R, 2012)

2-3. IMAGING PARAMETERS:

2-3-1. Image Quality:

- The four pillars of image quality are:-

1. Contrast to Noise Ratio (CNR)
2. Signal to Noise Ratio (SNR)
3. Spatial Resolution
4. Acquisition Time

2-3-2.Image Contrast and Weighting

Two Factors Affecting Image Contrast:-

1.Intrinsic Parameters : Those parameters that are inherent to the body's tissues and cannot be changed (T1 recovery, T2 decay, proton density, flow, apparent diffusion coefficients, perfusion, diffusion).

2.Extrinsic Parameters : Those parameters that can be changed via the imaging system (ex. TR, TE, flip angle, TI, echo train length, b value, FOV, matrix).

2-3-2-1.Types of Image Contrast:

The appearance of images is based on T1 contrast, T2 contrast, and proton density contrast.

1.T1 Contrast- When fat has high signal and appears bright, and water has low signal and appears dark.

2.T2 Contrast- When fat has low signal and appears dark, and water has high signal and appears bright.

3.Proton Density Contrast- Appears as a difference in signal intensities between tissues with varying hydrogen proton concentrations.

2-3-2-3.Types of Image Weighting:

- The amount of T1 or T2 contrast that has been allowed to influence an image will determine its weighting.

-T1 Weighted- Images in which weighting mainly depends on the differences between the T1 relaxation times of fat and water. The objective when trying to achieve T1 weighting is to prevent

recovery and prevent decay. This weighting is controlled by the TR (however a short TR and short TE are generally required).

-T2 Weighted- Images in which weighting mainly depends on the differences between the T2 decay times of fat and water. The objective when trying to achieve T2 weighting is to allow recovery and allow decay. This weighting is controlled by the TE (however a long TR and long TE are generally required).

-Proton (spin) Density Weighted- Images in which weighting mainly depends on the difference in the number of mobile hydrogen protons within adjacent tissues. The objective when trying to achieve PD weighting is to allow recovery and prevent decay. This weighting is controlled intrinsically by the amount of mobile hydrogen present in tissue (however a Long TR and short TE are generally required).

-4.T2* Weighting- Images in which weighting depends on the combination of T2decay and magnetic field inhomogeneities. This weighting is controlled by the TE (however a long TR and Long TE are generally required, as well as the use of a GE sequence)

2-3-3. Parameters:

- TR - The repetition time (TR) is the time between alpha pulses and is measured in milliseconds (ms). TR controls T1 weighting.
- TE - The echo time (TE) is the time between the alpha pulse and the peak of the echo, and is measured in milliseconds (ms). TE controls T2 weighting.
- TI - The time of inversion (TI) is a parameter used only in Inversion Recovery (IR)pulse sequences in order to null the signal from specific tissues (fat or fluid), and takes place between the 180° inversion pulse and the 90° alpha pulse. TI generally controls the amount of T1 contrast obtained during T1 weighted IR pulse sequence (along with TR), and which tissue signals will become nulled during T2 weighted IR pulse sequences.
- Number of Signals Averaged - The number of times that data is collected per TR period. NSA has a square root relationship with SNR, and a directly proportional relationship with scan time.
- Double NSA - If you double NSA, then you double scan time, but there is only a 41% increase in SNR.

- Quadruple NSA - If you quadruple NSA, then you quadruple scan time, and you get a 100% increase in signal.

- Flip Angle (Ernst Angle) - The angle of the NMV to the direction of the main magnetic field. Flip angle is controlled by the amplitude and duration of incoming RF pulses. Flip angles closer to 90O produce more signal.

- FOV - The area of anatomy that is covered in an image. This parameter has the greatest impact on SNR. FOV has a directly squared relationship to SNR.

  - Doubling the FOV - This gives you four times the signal.

  - Halving the FOV - This gives you one forth of the signal.

- Matrix - The number of pixels in the image. The matrix is identified by two numbers; phase matrix and frequency matrix.

  - Phase Matrix - The number of pixels in the phase direction. The phase matrix has a direct affect on time.

  - Frequency Matrix - The number of pixels in the frequency direction. The frequency matrix has no effect on time.

  - Number of Slices - This is limited by the TR selected and the system's SAR (Bossche, 2014)

2-4 MRI contrast:

Contrast agents are useful for detection of tumors, infection, inflammation, infarction and lesions. Contrast agents alter T1,T2, or T2* of various tissues, producing contrast.

Barium and iodine compounds are used to enhance contrast in xray procedures. These compounds are sometimes referred to as contrast “media” since their presence appears directly in the images.

MRI contrast is enhanced using contrast “agents” since the contrast is not directly imaged but rather the effect that the magnetic properties of the contrast agent has on the relaxation of tissues is imaged.

2-4-1.Contrast Agents:

Exogenous, Paramagnetic Agents, Superparamagnetic Agents, Ferromagnetic Agents, Positive Contrast Agents, Negative Contrast Agents, Route of Administration. (Allison, etal, 2007).

2-4-2.Contrast mechanisms in MRI:

2-4-2-1.Magnetization transfer contrast in MRI:

Magnetization transfer contrast (MTC) in magnetic resonance imaging (MRI) is the result of selectively observing the interaction of bulk water protons with the protons contained in macromolecules of a tissue. Since different tissues have different macromolecular compositions, the MTC can generate very high tissue contrast that is based on well-defined physiochemical properties. This is accomplished by combining a saturation transfer technique with standard MRI procedures. The specific practical and theoretical aspects of saturation transfer as it applies to the generation of MTC are reviewed and discussed. In the last 3 years, MTC has been applied to the study of the body, with useful applications demonstrated in evaluating the morphology of the knee joint, eye, brain, breast, and heart. The application of MTC to accentuate MR angiography and contrast agent studies has also been demonstrated. Thus, MTC is becoming another tool towards maximizing the quality and diagnostic potential of MRI. Recent studies on isolated macromolecules have suggested that the MTC effect is specific to the surface chemistry and correlation time of the macromolecules. These latter results indicate that the magnetization transfer process may provide a unique quantitative method of MR tissue characterization based on macromolecule dynamics and chemistry. (Balaban RS, etal, 1992)

2-5.The Brain:

The brain is one of the largest and most complex organs in the human body. It weighs approximately one pound at birth, and grows to about two pounds during childhood. The average female adult brain weighs about 2.7 pounds, while the average adult male brain weighs approximately three pounds.(Hitachi Medical Systems America, Inc).

The human brain is the central organ of the human nervous system, and with the spinal cord makes up the central nervous system. The brain consists of the cerebrum, the brainstem and the cerebellum. It controls most of the activities of the body, processing, integrating, and coordinating the information it receives from the sense organs, and making decisions as to the instructions sent to the rest of the body. The brain is contained in, and protected by, the skull bones of the head. The cerebrum is the largest part of the human brain. It is divided into two cerebral hemispheres. The cerebral cortex is an outer layer of grey matter, covering the core of white matter. The cortex is split into the neocortex and the much smaller allocortex. The neocortex is made up of six neuronal layers, while the allocortex has three or four. Each hemisphere is conventionally divided into four lobes.(www.wikipedia.org, 12-7-2017,2:30)

Magnetic resonance imaging (MRI) examinations of the brain can be performed with several coil types, depending on the design of the MRI unit and the information required. Traditionally, MRI examinations of the brain are performed with quadrature (i.e., circularly polarized) head coils. These volume coils are closely shaped around the head of the patient and usually present a so-called “bird-cage” configuration. Many coils are split in half, for easier patient access and positioning.(P. M. Parizel et al.2010)

Figure 2-14.Head/Spine Imaging (Owens, 2009)

2-5-2. Cerebrospinal Fluid (CSF):

Cerebrospinal fluid (CSF) is produced by a network of specialized cells called the choroid plexus. Choroid plexuses are found in the lining of all components of the ventricular system, except the anterior and posterior horns of the lateral ventricles, and the cerebral aqueduct. CSF is formed as plasma is filtered from the blood through the epithelial cells of the choroid plexus. These epithelial cells actively transport sodium, chloride, and bicarbonate ions into the ventricles,

with water following the resulting osmotic gradient. The choroid plexuses also act as a filtration system, removing metabolic waste, foreign substances, and excess neurotransmitters from the CSF. These networks have a very important role in helping to maintain the delicate extracellular environment required by the brain to function optimally.

CSF is produced at a rate of about 450 mL/day. At any given time, about 150 mL can be found within the CSF spaces. The volume of CFS in most adults is turned over approximately three times per day. CSF is constantly absorbed and replenished, with the brain maintaining the balance between production and absorption.

Besides providing chemical stability and nutrients needed by the brain, CSF provides buoyancy and support to the brain against gravity. The brain and CSF are similar in density, so the brain floats in neutral buoyancy, suspended in the CSF. This allows the brain to grow in size and weight without resting on the floor of the cranium, which would destroy nervous tissue. (Hitachi Medical Systems)

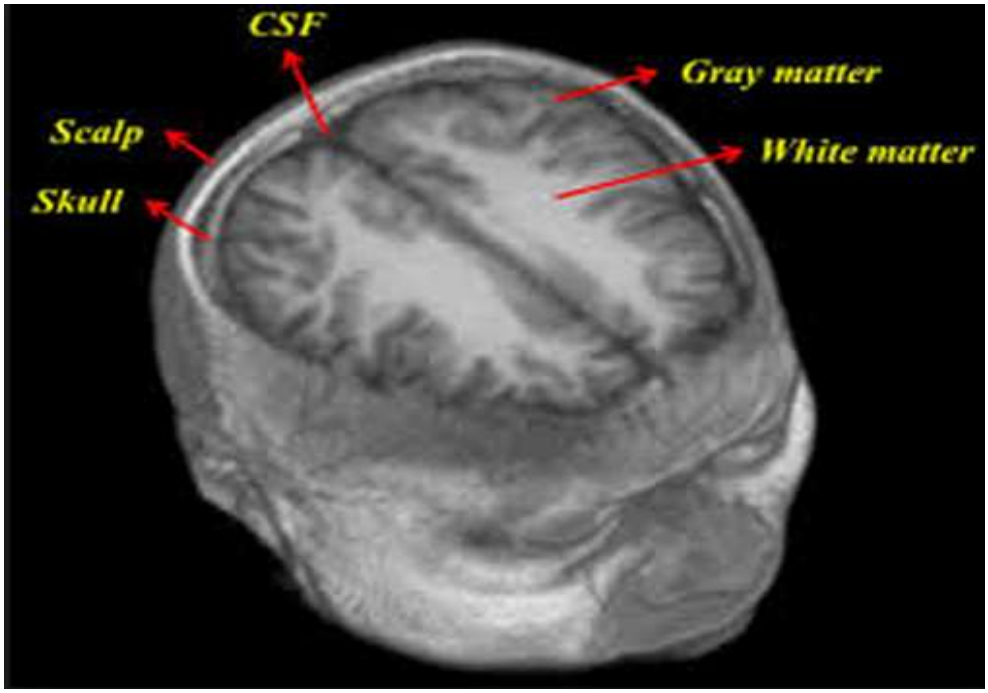

Figure 2-15.CSF,Gray matter, white matter

(Chuang CC, etal,2012)

2-5-3.brain magnetic resonance imaging:

MRI has evolved into an important diagnostic technique in medical imaging. However, reliability of the derived diagnosis can be degraded by artifacts, which challenge both radiologists and automatic computer-aided diagnosis. This work proposes a fully-automatic method for measuring image quality of three-dimensional (3D) structural MRI. Quality easures are derived by analyzing the air background of magnitude images and are capable of detecting image degradation from several sources, including bulk motion, residual agnetization from incomplete spoiling, blurring, and ghosting. The method has been validated on 749 3D T(1)-weighted 1.5T and 3T head scans acquired at 36 Alzheimer's Disease Neuroimaging Initiative (ADNI) study sites operating with various software and hardware combinations. Results are compared against qualitative grades assigned by the ADNI quality control center (taken as the reference standard). The derived quality indices are independent of the MRI system used and agree with the reference standard quality ratings with high sensitivity and specificity (>85%). The proposed procedures for quality assessment could be of great value for both research and routine clinical imaging. It could greatly improve workflow through its ability to rule out the need for a repeat scan while the patient is still in the magnet bore.(Mortamet B,etal,2009)

2-6. Previous Studies:

One hundred patients with CT-proven intracranial disease have been studied by magnetic resonance imaging (MRI) before and after intravenous injection with Gadolinium-DTPA (Gd-DTPA), in order to assess the role and clinical efficacy of Gd-DTPA. T2-weighted spin echo sequences, although sensitive to the detection of intracranial disease, in general fail to differentiate macroscopic tumour from oedema. Following Gd-DTPA, T1-weighted spin echo sequences in primary tumours demonstrated a variable degree of contrast enhancement unrelated to histological type. Small tumours, especially acoustic neuromas and meningiomas in the posterior fossa, were rendered more conspicuous. Optimum time for scanning was between five and 25 min following injection for all lesions except those adjacent to normal enhancing structures such as nasal/sinus mucosa and pituitary gland when delayed scans up to 45 min were necessary. No differences were observed between the 0.1 and 0.2 mmol/kg Gd-DTPA concentrations used and no complications attributable to Gd-DTPA were detected. Clinical advantages of Gd-DTPA include shorter scan times, macroscopic tumour/oedema separation and improved detection of certain tumors, particularly acoustic neuromas. (Stack,etal,1987).

Spin-lattice relaxation time T1 and relaxation parameters in magnetization transfer (MT) imaging were measured in 11 intracranial tumors before and after injection of Gd-DTPA at 0.1 T by using the inversion recovery method and the saturation transfer technique, respectively. Pre injection T1 relaxation times of the tumors were longer than those of white matter, but after Gd-enhancement the relaxation times of most tumors were in the same range as those of white matter. Gd-DTPA shortened the apparent relaxation time in the presence of off-resonance saturation pulse (T1α) due to marked shortening of the relaxation time of mobile water (T1w). Gd-DTPA decreased the magnetization transfer contrast (MTC) but did not influence on the magnetization transfer rate (Rwm). The parameters MTC and Rwm differed clearly between Gd-enhanced tumors and normal brain, whereas the relaxation time T1α was in many Gd-enhanced tumors in the same range as in normal brain.(Kurk,etal,1995)

This review focuses on MRI contrast agents for tumor diagnosis. Several types of low molecular weight Gd3+-based complexes and dextran-coated superparamagnetic iron oxide (SPIO) nanoparticles have been used for clinical tumor diagnosis as longitudinal relaxation time (T1) and transverse relaxation time (T2) MRI contrast agents, respectively. To further improve the sensitivity of MRI, new types of chelates for T1 MRI contrast agents and combination of low molecular weight T1 MRI contrast agents with different types of carriers have been investigated. Different types of materials for forming secure coating layers of SPIO and novel superparamagnetic particles with higher relaxivity values have been explored. Various types of ligands were applied to improve the capability to target tumor for both T1 and T2 contrast agents.(Cheng, etal, 2012)

Chapter three

Chapter Three

Materials and methods

This descriptive study, about the brain, the mean objective was to study the brain MRI image quality pre and post- administration of contrast media, the data were collected from MRI department of Antalya Medical Center, and the study was carried out in the (Sudan Khartoum State) between July 2017 and October 2017.

3-1. material:

3-1-1.Study sample:

The patient population consist of 63 (32 female, 31 male) with age ranging from (8- 90)Years, patients scheduled for Brain lesion at Antalya medical center participated in this study.

3-1-2. Machine used:

The machine used 1.5 Tesla scanners GE (general electrical)closed permanent magnet unit.

3-2.Methods:

3-2.1.Techniqe used:

All imaging was carried out with a 1.5 Tesla superconducting system using a standard quadrature head coil.

Imaging parameters of contrast-enhanced T1W imaging were TR, TE:

	TR.PRE	TE.PRE	TR.POST	TE.POST
1	520	12	520	12
2	520	11	520	11
3	190	5.1	190	5.1
4	190	5	190	5
5	190	4.2	190	4.2
6	190	4.1	190	4.1

Table (3-1). Imaging parameters -TR, TE

FOV: 230 mm, Image Matrix: (512 × 512), (256 × 256), slice thickness: 5 mm,
Slice interval: 1.5 mm, phase encoding direction, and R to L and acquisition time: 3 min 48 seconds, Sequences: Axial T1.

All patients received intravenous gadolinium contrast medium (the dose of which was decided according to weight of the patient) given by a computer-controlled injector at rate of 0.2 ML/second.

3-2-2.Method of measurement:

The imaging protocol included acquisition of pre- and post-contrast-enhanced T1-weighted (T1WI).

The MRI images of pre- post contrast T1WI were obtained in axial were evaluated by simple visual inspection by experienced radiologist and attention was paid to determine the presence or absence and the location of pathological.

The mean signal intensity (SI) was measured for each tissue type (white matter, gray matter, CSF, lesion) both pre- and post-Contrast using software (RadiAnt DICOM Viewer (32-bit)).

Structures were traced manually by computer cursor and area of interest were calculated. Same imaging plane used before and after contrast media injection.

The appearance of the cases evaluated to determine the signal intensities pre contrast for (CSF, white matter, gray matter and Lesion) compared to post contrast (CSF, white matter, gray matter and Lesion) using approach measuring the signal intensities, this data was then recorded and tabulated by the researcher.

3-2-3. Problem and methods used:

The researcher encountered the problem of varying of position (the position change a little pre and post the contrast according to the patient motion) figure (3-1).

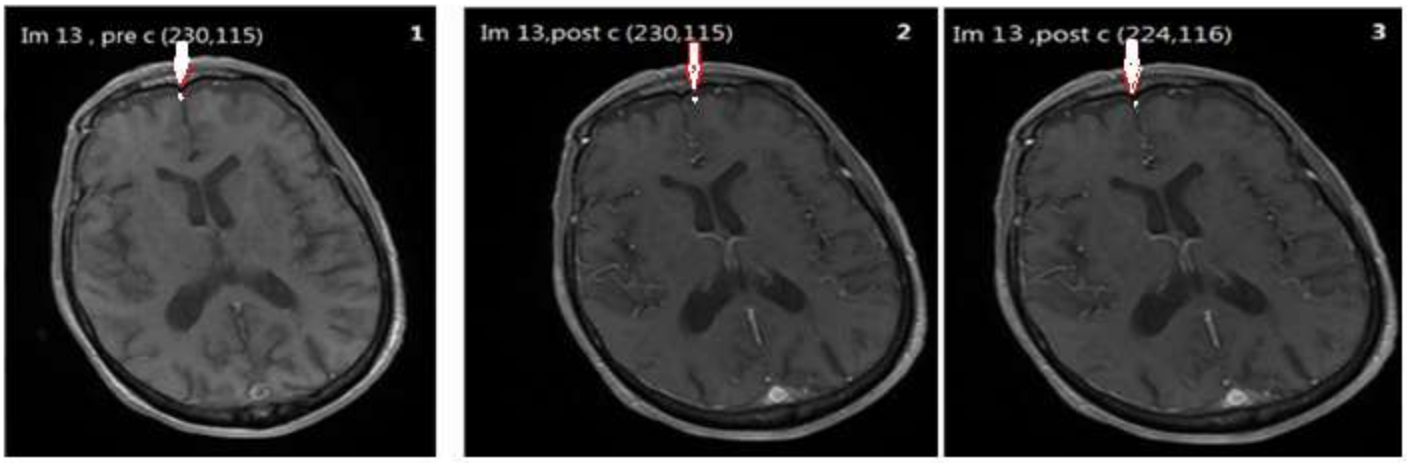

Figure (3-1) varying of position- Same imaging plane

Method which the researcher used to solve the problem:

-Selection of a clear point in the same imaging plane before and after contrast media injection according to the points shown on figure (3-2).

- Selection of measurement points next to a clear landmark on the image.

-By subtracting the coordinates of the two points then the difference in taking the reading of signal intensity was applied.

Example:-

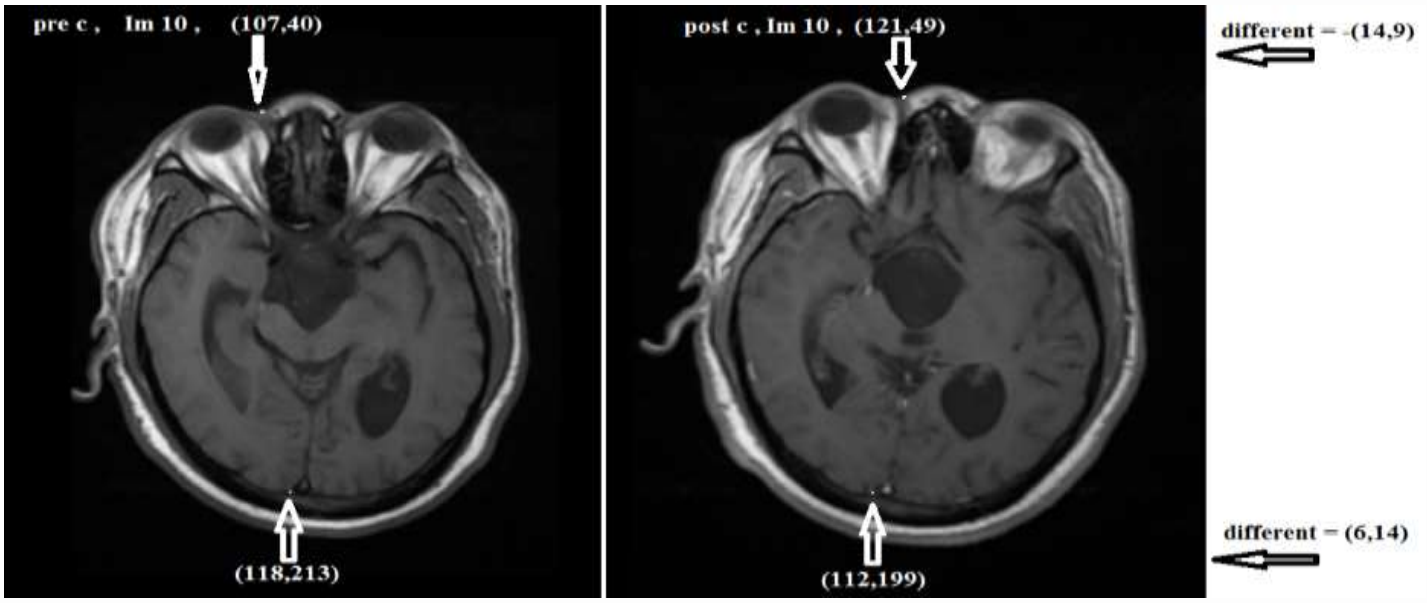

Figure (3-2) same imaging plane- compare its coordinates

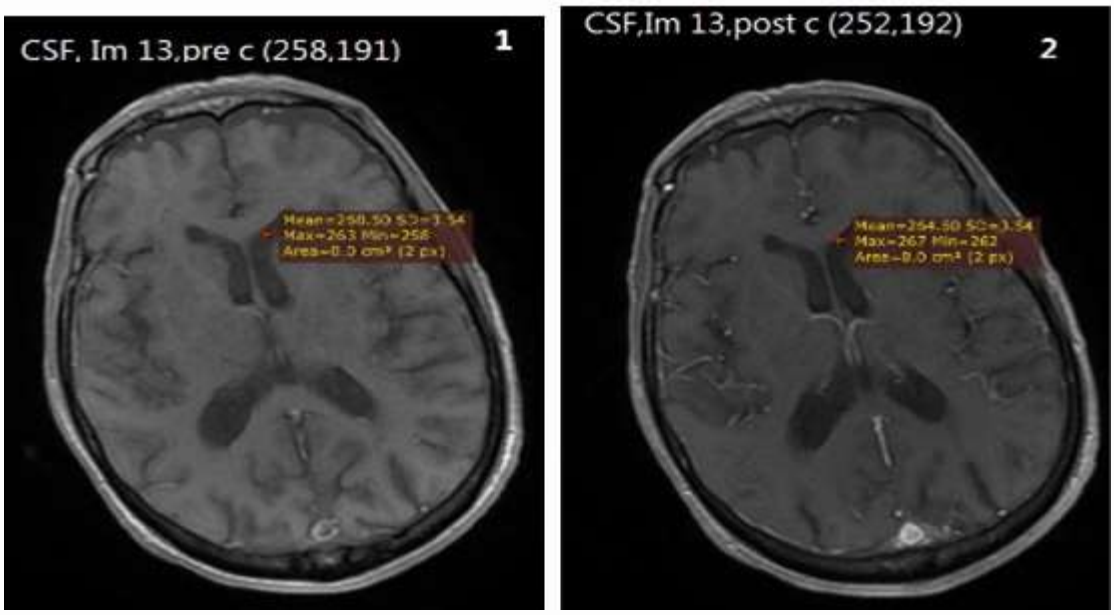

Figure (3-3) measure CSF- Same imaging plane

3-2-4.Data collection:

The data were collected from MRI department of Antalya medical center, the study was carried out in the (Sudan Khartoum State).

The measurement was taken using the software (RadiAnt DICOM Viewer (32-bit)).

3-7.Data analysis:

Exel program and SPSS T-Test was used in the analysis of data.

3-8. Ethical Consideration:

The data available were used only for the purposes of the study and not used by any other person and the patients privacy was respected.

Chapter Four

Chapter Four

Results

Table 4.1: distribution of participants with respect to age:

Age	Frequency	Percentage
Less than 10 years	5	7.9
10-20 years	9	14.3
21-30 years	11	17.5
31-40 years	7	11.1
41-50 years	9	14.3
51-60 years	10	15.9
More than 60 years	12	19.0
Total	**63**	**100.0**

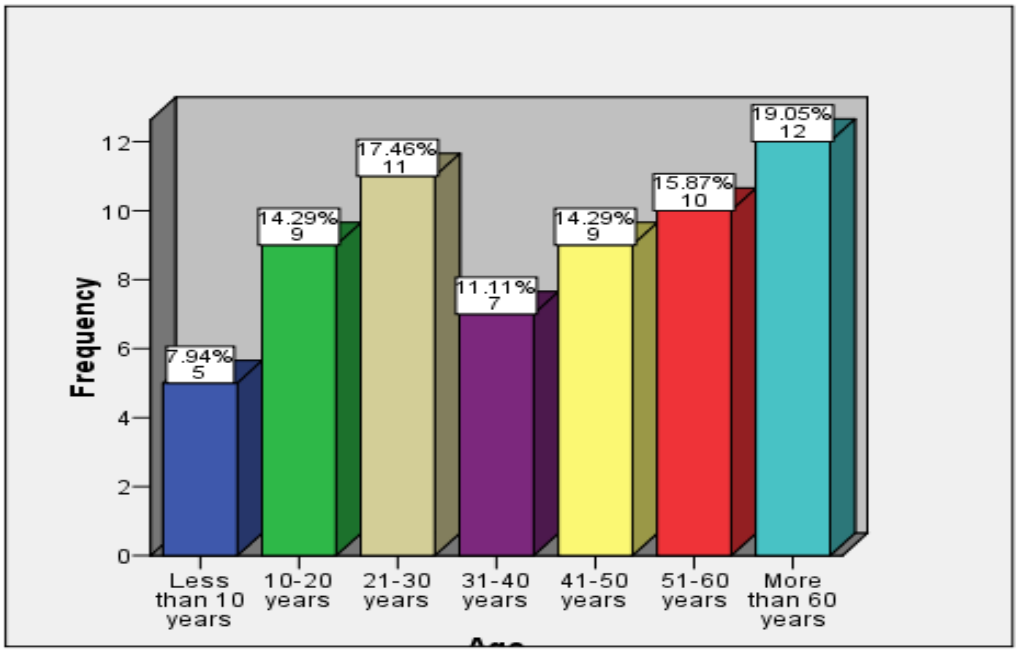

Figure 4.1: distribution of participants with respect to age

Table 4.2: distribution of participants with respect to gender:

Gender	Frequency	Percent
Male	31	49.2
Female	32	50.8
Total	**63**	**100.0**

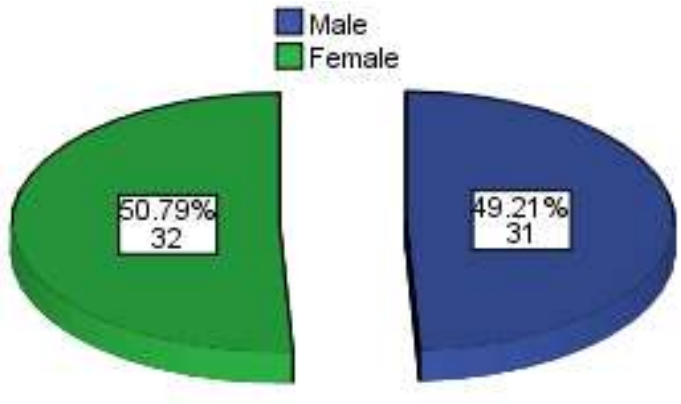

Figure 4.2: distribution of participants with respect to gender

Table 4.3: Mean signal intensity (CSF) for pre-contrast and post-contrast:

	Mean	Std. Deviation	Std. Error Mean
PRE- contrast	193.294	32.6261	4.1105
POST- contrast	198.704	39.8450	5.0200

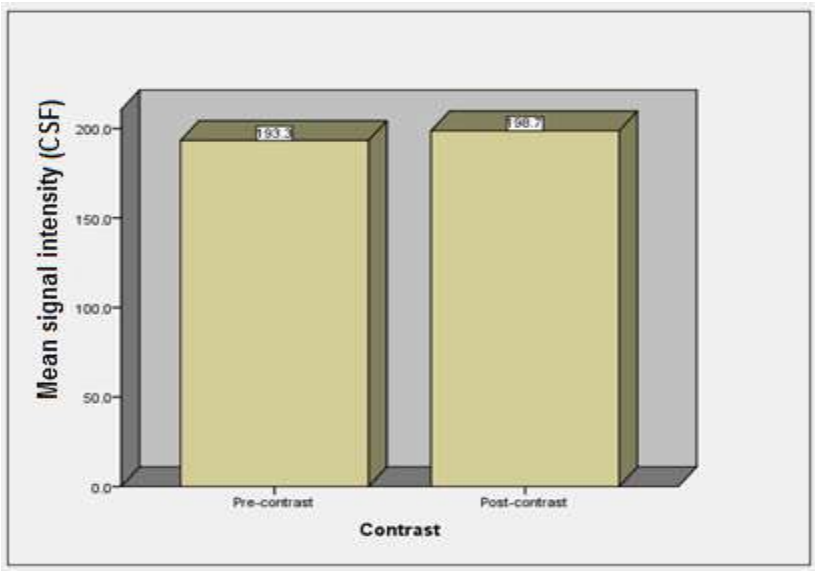

Figure 4.3: Mean signal intensity (CSF) for pre-contrast and post-contrast

Table 4.4: Paired Samples t-test for Equality of Means signal intensity of pre-contrast and post-contrast (CSF):

Paired Differences						
	Mean	Std. Deviation	Std. Error Mean	T	Df	Sig. (2-tailed)
Pre- contrast - **Post-** contrast	-5.4100	16.7214	2.1067	-2.568	62	.013

Table 4.5: Mean signal intensity (white matter) for pre-contrast and post-contrast:

	Mean	**Std. Deviation**	**Std. Error Mean**
Pre-contrast	437.100	42.3561	5.3364
Post-contrast	452.267	44.0434	5.5489

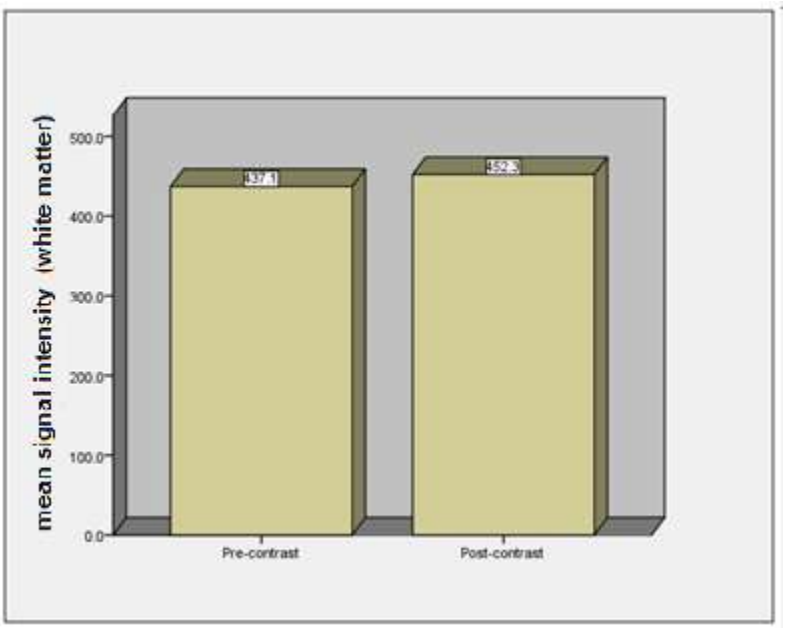

Figure 4.4: Mean signal intensity (white matter) for pre-contrast and post-contrast

Table 4.6: Paired Samples t-test for Equality of Means signal intensity of pre-contrast and post-contrast:

Paired Differences						
	Mean	Std. Deviation	Std. Error Mean	t	Df	Sig. (2-tailed)
Pre-white matter - Post-white matter	-1.5167	17.1736	2.1637	-7.010	62	.000

Table 4.7: Mean signal intensity (gray matter) for pre-contrast and post-contrast:

	Mean	**Std. Deviation**	**Std. Error Mean**
Pre-contrast	361.413	56.1329	7.0721
Post-contrast	386.235	56.2481	7.0866

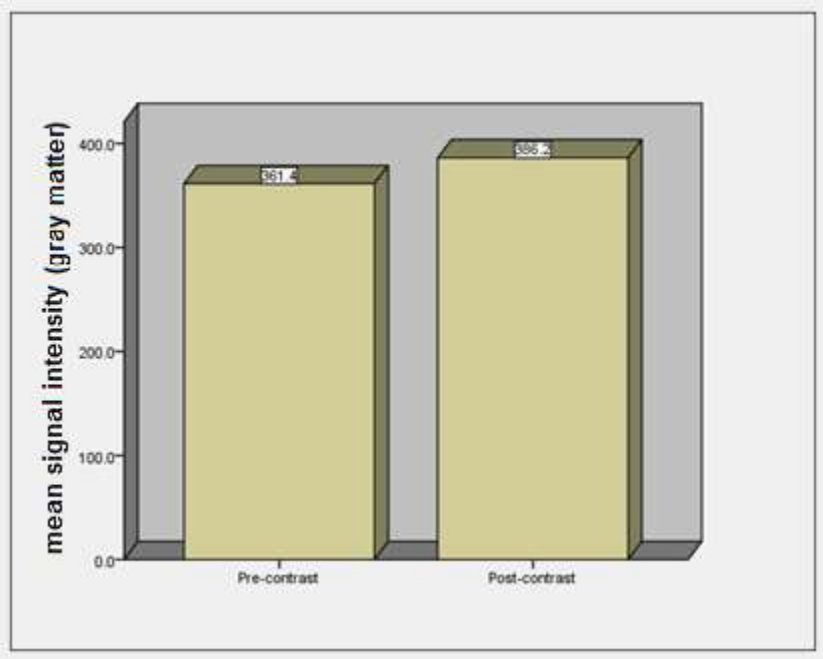

Figure 4.5: Mean signal intensity (gray matter) for pre-contrast and post-contrast

Table 4.8: Paired Samples t-test for Equality of Means signal intensity of pre-contrast and post-contrast (gray matter):

Paired Differences						
	Mean	Std. Deviation	Std. Error Mean	t	Df	Sig. (2-tailed)
Pre- contrast - **Post-** contrast	-2.4823	22.6024	2.8476	-8.717	62	.000

Table 4.9: Mean signal intensity (Lesion) for pre-contrast and post-contrast:

	Mean	**Std. Deviation**	**Std. Error Mean**
Pre- contrast	346.397	194.5113	24.5061
Post- contrast	546.390	332.0755	41.8376

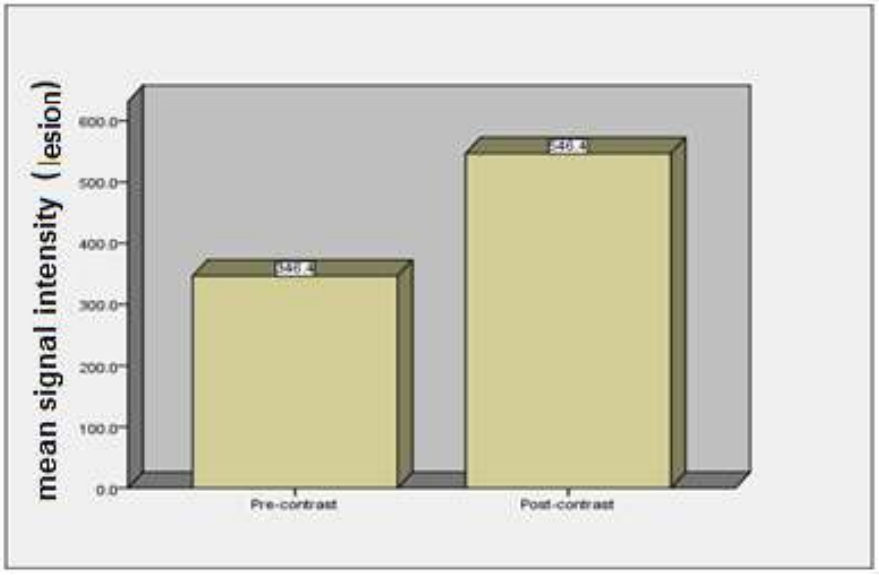

Figure 4.6: Mean signal intensity (Lesion) for pre-contrast and post-contrast

Table 4.10: Paired Samples t-test for Equality of Means signal intensity (Lesion) of pre-contrast and post-contrast:

Paired Differences						
	Mean	Std. Deviation	Std. Error Mean	t	Df	Sig. (2-tailed)
Pre- contrast – **Post-** contrast	-1.9999	206.9424	26.0723	-7.671	62	.000

Table 4.11: Mean signal intensity (CSF) for pre-contrast and post-contrast with respect to age:

Age		Mean	Std. Deviation	Std. Error Mean
Less than 10 years	Pre- contrast	203.600	68.7908	30.7642
	Post-contrast	212.700	69.3394	31.0095
10-20 years	Pre- contrast	177.833	25.1794	8.3931
	Post- contrast	181.667	32.2519	10.7506
21-30 years	Pre- contrast	192.455	31.2686	9.4278
	Post- contrast	194.848	29.9048	9.0166
31-40 years	Pre- contrast	199.071	24.1099	9.1127
	Post- contrast	202.857	31.7841	12.0132
41-50 years	Pre- contrast	205.389	28.8485	9.6162
	Post- contrast	219.278	59.9552	19.9851
51-60 years	Pre- contrast	187.350	27.8548	8.8085
	Post- contrast	189.750	30.3143	9.5862
More than 60 years	Pre- contrast	193.875	30.8848	8.9157
	Post- contrast	198.792	30.6887	8.8591

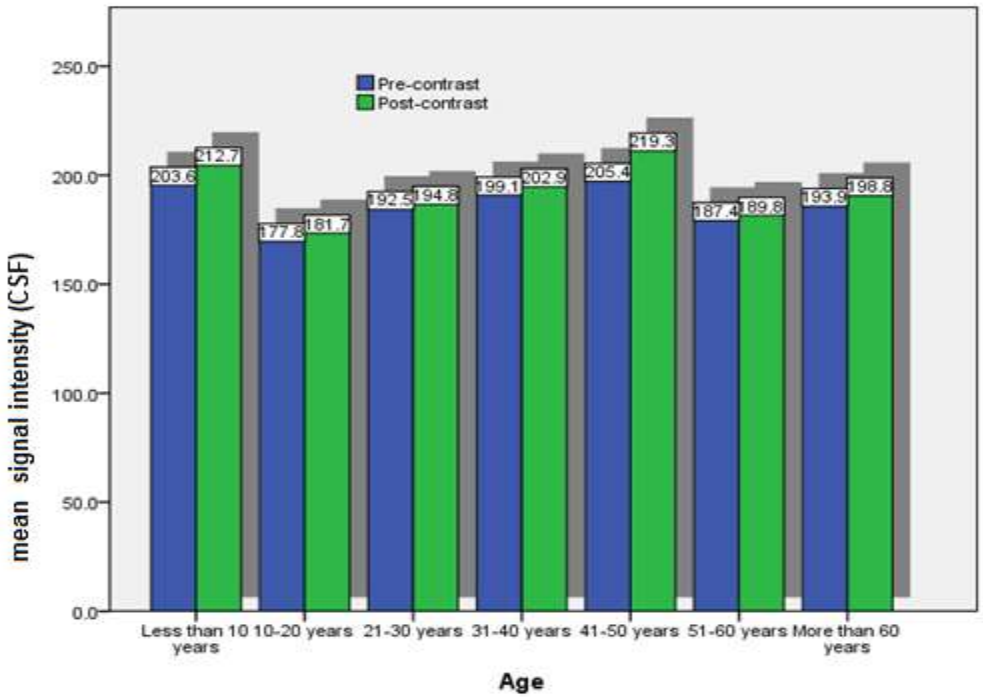

Figure 4.7: Mean signal intensity (CSF) for pre-contrast and post-contrast with respect to age**.**

Table 4.12: Paired Samples t-test for Equality of Means signal intensity (CSF) of pre-contrast and post-contrast with respect to age:

Age		Paired Differences					
		Mean	Std. Deviation	Std. Error Mean	T	Df	Sig. (2-tailed)
Less than 10 years	Pre-C - Post-C	-9.1000	14.8762	6.6528	-1.368	4	.243
10-20 years	Pre-C - Post-C	-3.8333	12.2551	4.0850	-.938	8	.376
21-30 years	Pre-C - Post-C	-2.3936	12.0504	3.6333	-.659	10	.525
31-40 years	Pre-C - Post-C	-3.7857	12.1204	4.5811	-.826	6	.440
41-50 years	Pre-C - Post-C	-1.3889	36.8619	12.2873	-1.130	8	.291
51-60 years	Pre-C - Post-C	-2.4000	6.7692	2.1406	-1.121	9	.291
More than 60 years	Pre-C - Post-C	-4.9167	7.8793	2.2746	-2.162	11	.054

Table 4.13: Mean signal intensity (white matter) for pre-contrast and post-contrast with respect to age:

Age		Mean	Std. Deviation	Std. Error Mean
Less than 10 years	Pre- contrast	429.900	52.8611	23.6402
	Post- contrast	454.900	48.1799	21.5467
10-20 years	Pre- contrast	431.056	60.8011	20.2670
	Post- contrast	443.833	65.0380	21.6793
21-30 years	Pre- contrast	451.273	37.5609	11.3250
	Post- contrast	470.864	43.1510	13.0105
31-40 years	Pre- contrast	438.857	28.6643	10.8341
	Post- contrast	456.404	36.3435	13.7365
41-50 years	Pre- contrast	451.222	46.5088	15.5029
	Post- contrast	460.833	47.9088	15.9696
51-60 years	Pre- contrast	415.783	33.5893	10.6219
	Post- contrast	428.800	29.0719	9.1934
More than 60 years	Pre- contrast	437.792	36.7030	10.5952
	Post- contrast	451.167	35.4832	10.2431

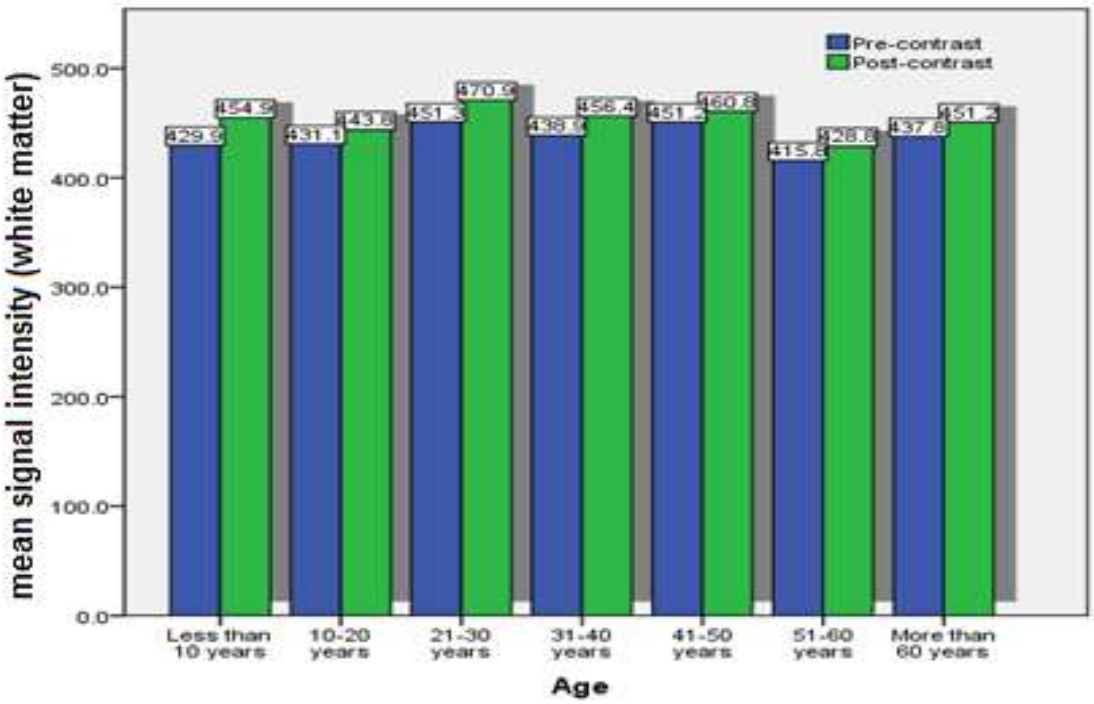

Figure 4.8: Mean signal intensity (white matter) for pre-contrast and post-contrast with respect to age

Table 4.14: Paired Samples t-test for Equality of Means of signal intensity (white matter) pre-contrast and post-contrast with respect to age:

Age		Paired Differences					
		Mean	Std. Deviation	Std. Error Mean	t	df	Sig. (2-tailed)
Less than 10 years	Pre-C-Post-C	-0.25000	19.4454	8.6963	-2.875	4	.045
10-20 years	Pre-C-Post-C	-0.12778	13.7138	4.5713	-2.795	8	.023
21-30 years	Pre-C-Post-C	-0.19591	22.4787	6.7776	-2.891	10	.016
31-40 years	Pre-C-Post-C	-0.17547	17.5279	6.6249	-2.649	6	.038
41-50 years	Pre-C-Post-C	-9.6111	9.3199	3.1066	-3.094	8	.015
51-60 years	Pre-C-Post-C	-1.3017	10.8026	3.4161	-3.811	9	.004
More than 60 years	Pre-C-Post-C	-1.3375	22.3099	6.4403	-2.077	11	.062

Table 4.15: Mean signal intensity (gray matter) for pre-contrast and post-contrast with respect to age:

Age		Mean	Std. Deviation	Std. Error Mean
Less than 10 years	Pre- contrast	369.400	60.5221	27.0663
	Post- contrast	389.500	53.4088	23.8851
10-20 years	Pre- contrast	354.778	88.0331	29.3444
	Post- contrast	382.000	86.1184	28.7061
21-30 years	Pre- contrast	374.273	39.6997	11.9699
	Post- contrast	395.864	28.6689	8.6440
31-40 years	Pre- contrast	375.143	52.1790	19.7218
	Post- contrast	409.333	63.9482	24.1701
41-50 years	Pre- contrast	382.500	70.4459	23.4820
	Post- contrast	403.667	74.4916	24.8305
51-60 years	Pre- contrast	355.700	33.7361	10.6683
	Post- contrast	366.950	30.6798	9.7018
More than 60 years	Pre- contrast	332.208	40.7294	11.7576
	Post- contrast	368.750	47.3932	13.6812

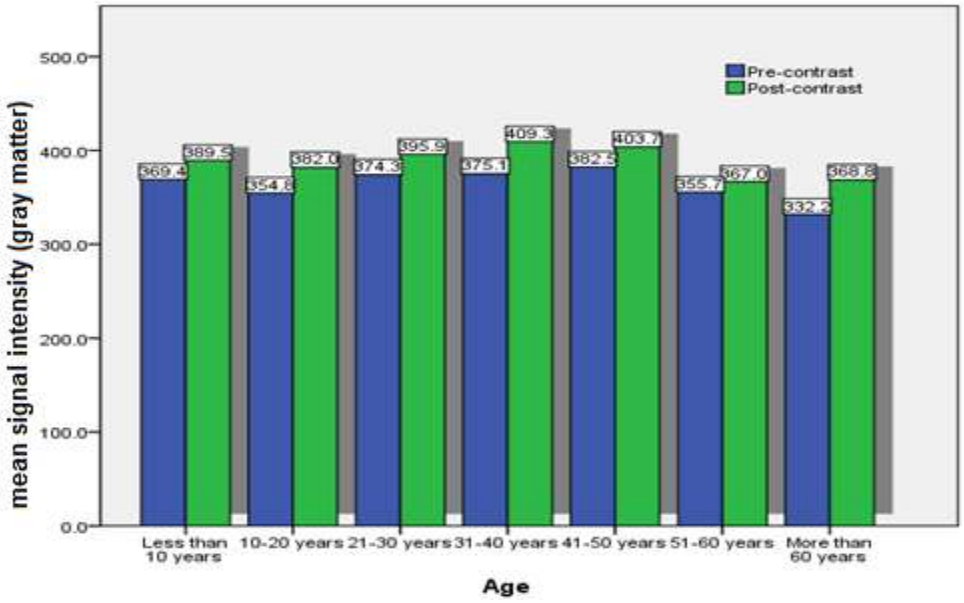

Figure 4.9: Mean signal intensity (gray matter) for pre-contrast and post-contrast with respect to age.

Table 4.16: Paired Samples t-test for Equality of Means signal intensity (gray matter) of pre-contrast and post-contrast with respect to age:

Age		Paired Differences					
		Mean	Std. Deviation	Std. Error Mean	t	df	Sig. (2-tailed)
Less than 10 years	Pre-CE-Post-CE	-0.20100	12.5120	5.5955	-3.592	4	.023
10-20 years	Pre-CE-Post-CE	-0.27222	26.2668	8.7556	-3.109	8	.014
21-30 years	Pre-CE-Post-CE	-0.21591	21.8333	6.5830	-3.280	10	.008
31-40 years	Pre-CE-Post-CE	-0.34190	25.6481	9.6941	-3.527	6	.012
41-50 years	Pre-CE-Post-CE	-2.1167	12.8962	4.2987	-4.924	8	.001
51-60 years	Pre-CE-Post-CE	-1.1250	17.1290	5.4167	-2.077	9	.068
More than 60 years	Pre-CE-Post-CE	-3.6542	27.5355	7.9488	-4.597	11	.001

Table 4.17: Mean signal intensity (Lesion) for pre-contrast and post-contrast with respect to age:

Age		Mean	Std. Deviation	Std. Error Mean
Less than 10 years	Pre- contrast	455.300	95.2638	42.6033
	Post- contrast	626.500	192.3548	86.0237
10-20 years	Pre- contrast	295.722	300.3228	100.1076
	Post- contrast	565.833	526.3289	175.4430
21-30 years	Pre- contrast	406.000	170.9987	51.5580
	Post- contrast	620.659	224.6388	67.7312
31-40 years	Pre- contrast	321.357	265.7520	100.4448
	Post- contrast	413.357	373.5929	141.2048
41-50 years	Pre- contrast	301.333	132.7564	44.2521
	Post- contrast	509.667	315.3900	105.1300
51-60 years	Pre- contrast	323.000	188.3320	59.5558
	Post- contrast	542.850	361.0185	114.1641
More than 60 years	Pre- contrast	352.292	154.1803	44.5080
	Post- contrast	538.444	290.5974	83.8882

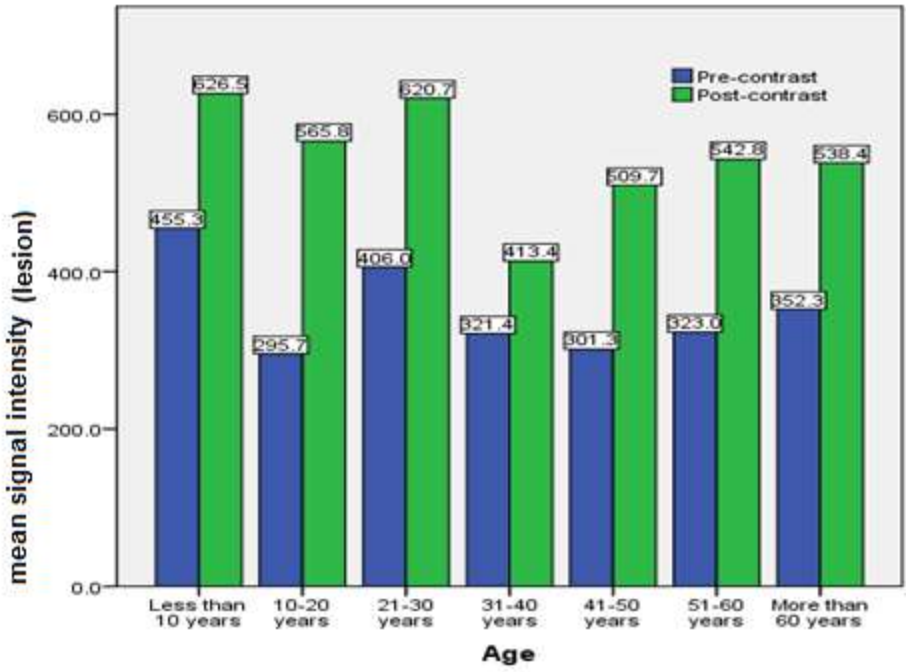

Figure 4.10: Mean signal intensity (Lesion) for pre-contrast and post-contrast with respect to age.

Table 4.18: Paired Samples t-test for Equality of Means of signal intensity (Lesion) pre-contrast and post-contrast with respect to age:

Age		Paired Differences					
		Mean	Std. Deviation	Std. Error Mean	t	df	Sig. (2-tailed)
Less than 10 years	Pre-CE - Post-CE	-1.7120	146.9152	65.7025	-2.606	4	.060
10-20 years	Pre-CE - Post-CE	-2.7011	256.4026	85.4675	-3.160	8	.013
21-30 years	Pre-CE - Post-CE	-2.1466	215.4635	64.9647	-3.304	10	.008
31-40 years	Pre-CE - Post-CE	-9.2000	167.1294	63.1690	-1.456	6	.196
41-50 years	Pre-CE - Post-CE	-2.0833	218.1692	72.7231	-2.865	8	.021
51-60 years	Pre-CE - Post-CE	-2.1985	242.8003	76.7802	-2.863	9	.019
More than 60 years	Pre-CE - Post-CE	-1.8615	181.0150	52.2545	-3.562	11	.004

.

Table 4.19: Mean signal intensity (CSF) for pre-contrast and post-contrast with respect to gender:

Gender		Mean	Std. Deviation	Std. Error Mean
Male	pre-contrast	201.871	36.7153	6.5943
	post- contrast	203.258	38.7360	6.9572
Female	pre- contrast	184.984	26.0683	4.6083
	post- contrast	194.292	41.0162	7.2507

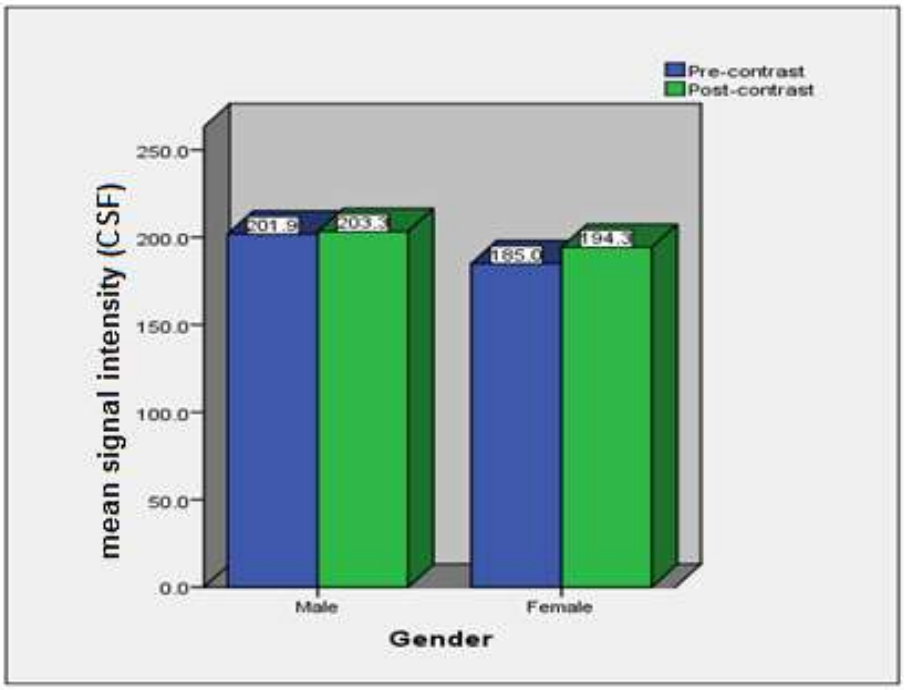

Figure 4.11: Mean signal intensity (CSF) for pre-contrast and post-contrast with respect to gender.

Table 4.20: Paired Samples t-test for Equality of Means signal intensity (CSF) of pre-contrast and post-contrast with respect to gender:

Gender		Paired Differences					
		Mean	Std. Deviation	Std. Error Mean	t	df	Sig. (2-tailed)
Male	Pre-C - POST-C	-1.3871	8.9951	1.6156	-.859	30	.397
Female	Post-C - POST-C	-9.3072	21.1907	3.7460	-2.485	31	.019

Table 4.21: Mean signal intensity (white matter) for pre-contrast and post-contrast with respect to gender:

Gender		Mean	Std. Deviation	Std. Error Mean
Male	Pre-white matter	452.333	39.2932	7.0573
	Post-white matter	467.758	37.7781	6.7851
Female	Pre-white matter	422.344	40.4611	7.1526
	Post-white matter	437.260	45.0118	7.9570

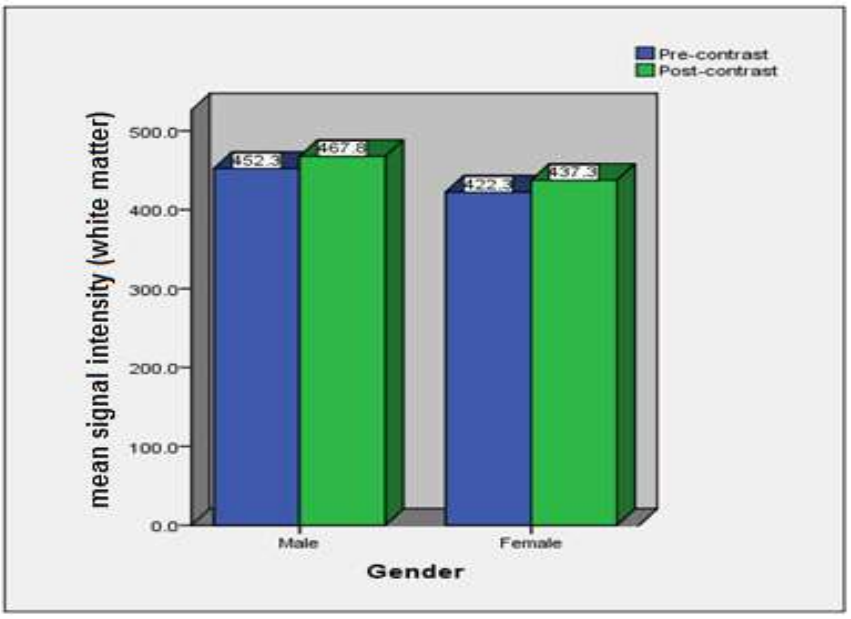

Figure 4.12: Mean signal intensity (white matter) for pre-contrast and post-contrast with respect to gender.

Table 4.22: Paired Samples t-test for Equality of Means signal intensity (white matter) of pre-contrast and post-contrast with respect to gender:

Gender		Paired Differences					
		Mean	Std. Deviation	Std. Error Mean	t	df	Sig. (2-tailed)
Male	Pre-C - Post-C	-1.5425	17.6319	3.1668	-4.871	30	.000
Female	Pre-C - Post-C	-1.4917	16.9965	3.0046	-4.965	31	.000

Table 4.23: Mean signal intensity (gray matter) for pre-contrast and post-contrast with respect to gender:

Gender		**Mean**	**Std. Deviation**	**Std. Error Mean**
Male	Pre- contrast	371.774	70.2607	12.6192
	Post contrast	400.661	70.0776	12.5863
Female	Pre- contrast	351.375	36.2369	6.4058
	Post- contrast	372.260	34.1398	6.0351

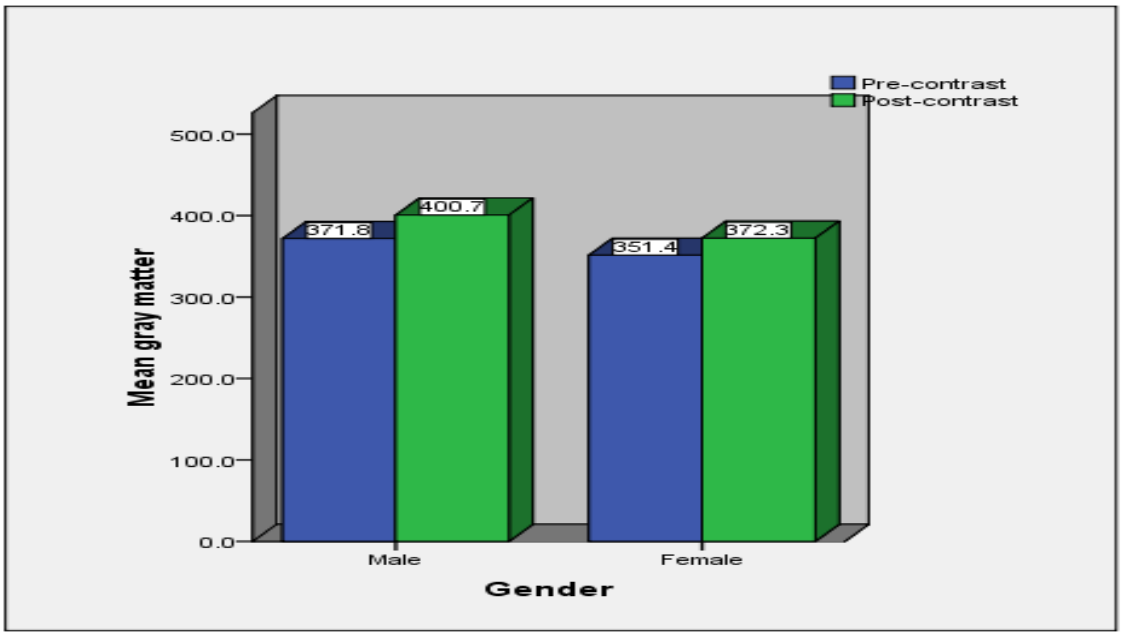

Figure 4.13: Mean signal intensity (gray matter) for pre-contrast and post-contrast with respect to gender.

Table 4.24: Paired Samples t-test for Equality of Means signal intensity (gray matter) of pre-contrast and post-contrast with respect to gender:

Gender		Paired Differences					
		Mean	Std. Deviation	Std. Error Mean	t	df	Sig. (2-tailed)
Male	Pre-C - Post-C	-2.8887	28.9559	5.2006	-5.555	30	.000
Female	Pre-C - Post-C	-2.0885	13.3348	2.3573	-8.860	31	.000

Table 4.25: Mean signal intensity (Lesion) for pre-contrast and post-contrast with respect to gender:

Gender		**Mean**	**Std. Deviation**	**Std. Error Mean**
Male	Pre- **contrast**	321.032	182.3488	32.7508
	Post- **contrast**	485.027	320.7761	57.6131
Female	Pre- **contrast**	370.969	205.4853	36.3250
	Post- **contrast**	605.836	336.9821	59.5706

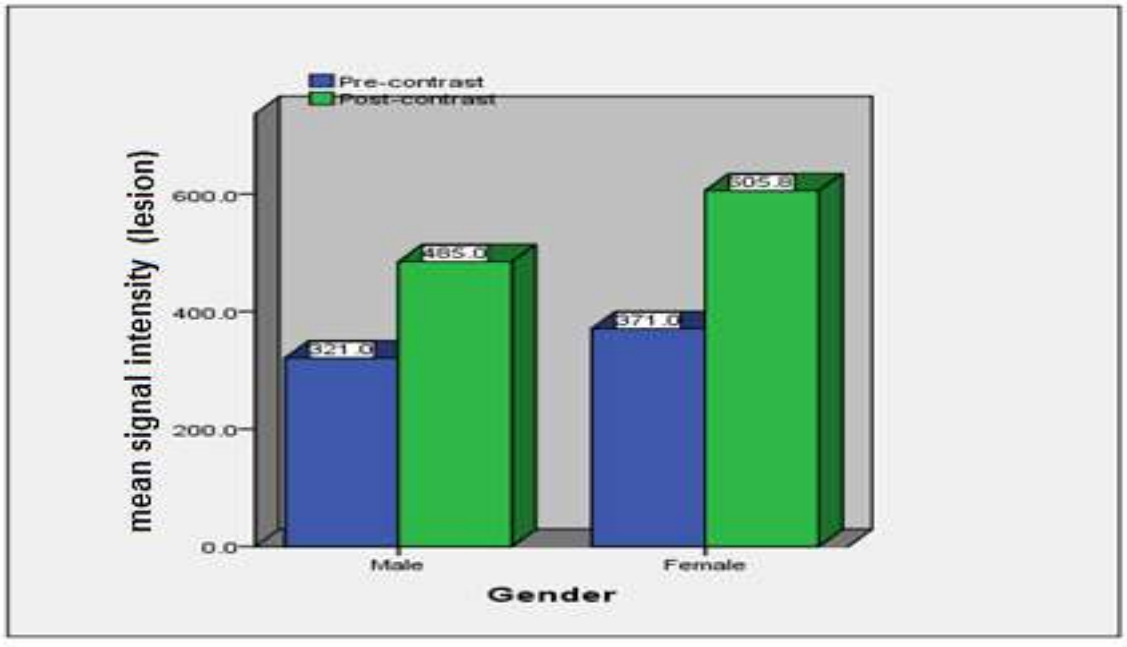

Figure 4.14: Mean signal intensity (Lesion) for pre-contrast and post-contrast with respect to gender.

Table 4.26: Paired Samples t-test for Equality of Means signal intensity (Lesion) of pre-contrast and post-contrast with respect to gender:

Gender		Paired Differences					
		Mean	Std. Deviation	Std. Error Mean	t	df	Sig. (2-tailed)
Male	Pre-CE - Post-CE	-1.6399	196.8284	35.3514	-4.639	30	.000
Female	Pre-CE- Post-CE	-2.3487	213.5587	37.7522	-6.221	31	.000

Table 4.27: distribution of participants with respect to their diagnosis:

	Frequency	**Percentage**
tumor	39	61.9
Brain infection	5	7.9
Normal	9	14.3
Atrophy	1	1.6
Benign	9	14.3
Total	**63**	**100.0**

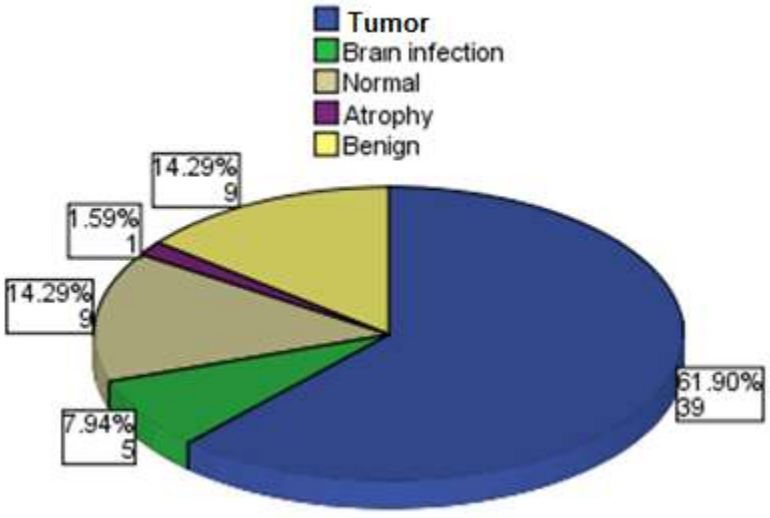

Figure 4.15: distribution of participants with respect to diagnosis

Table (4.28): Chi-square test for association of diagnosis and age:

		Diagnose									
		tumor		Brain infection		Normal		Atrophy		Benign	
		Count	N %	Count	N %	Count	N %	Count	N %	Count	N %
Age	Less than 10 years	5	100.0%	0	.0%	0	.0%	0	.0%	0	.0%
	10-20 years	8	88.9%	0	.0%	1	11.1%	0	.0%	0	.0%
	21-30 years	6	54.5%	3	27.3%	2	18.2%	0	.0%	0	.0%
	31-40 years	3	42.9%	0	.0%	3	42.9%	0	.0%	1	14.3%
	41-50 years	5	55.6%	1	11.1%	0	.0%	0	.0%	3	33.3%
	51-60 years	4	40.0%	1	10.0%	2	20.0%	1	10.0%	2	20.0%
	More than 60 years	8	66.7%	0	.0%	1	8.3%	0	.0%	3	25.0%

Pearson Chi-Square Tests		
	Diagnose	
Age	Chi-square	30.641
	Df	24
	Sig.	0.164

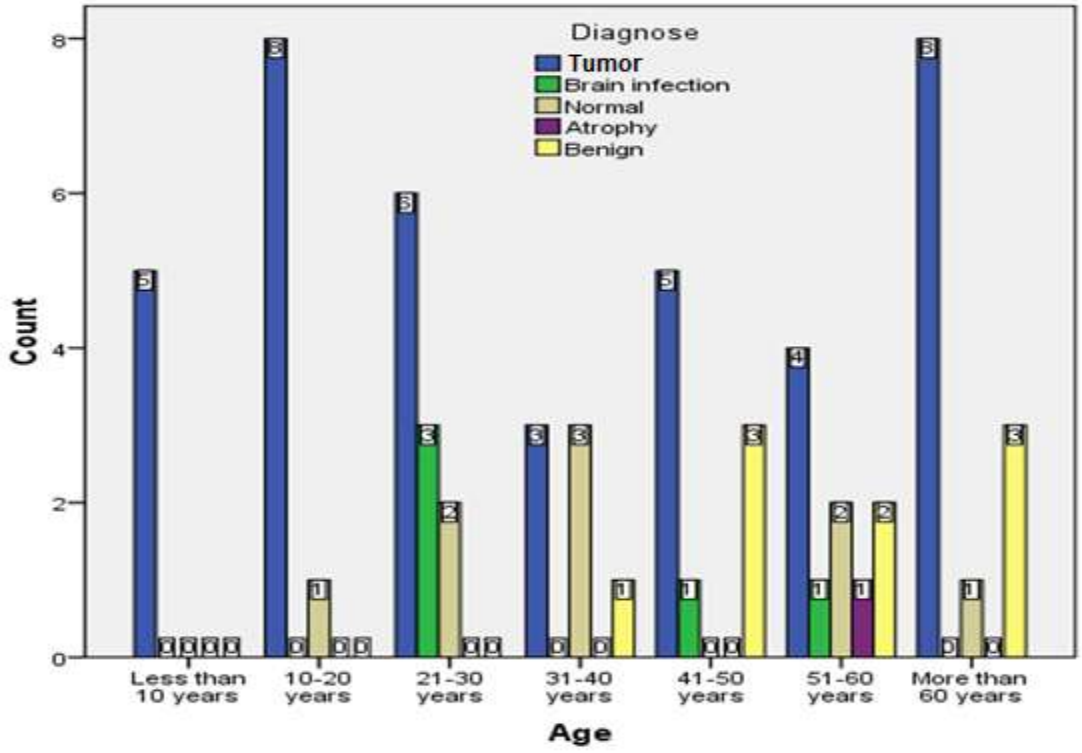

Figure 4.16: distribution of diagnosis with respect to age

Table (4.29): Chi-square test for association of diagnosis and gender:

		Diagnose									
		tumor		Brain infection		Normal		Atrophy		Benign	
		Count	N %	Count	N %	Count	N %	Count	N %	Count	N %
Gender	Male	19	61.3%	3	9.7%	3	9.7%	1	3.2%	5	16.1%
	Female	20	62.5%	2	6.2%	6	18.8%	0	.0%	4	12.5%

Pearson Chi-Square Tests		
	Diagnose	
Gender	Chi-square	2.321
	Df	4
	Sig.	0.677

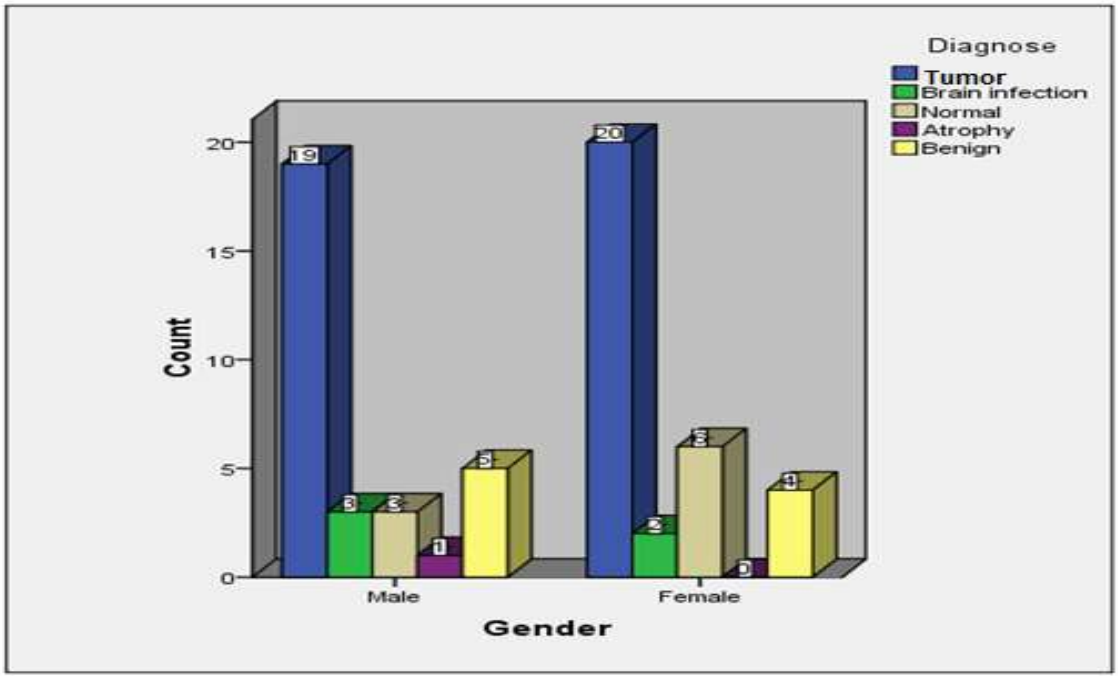

Figure 4.17: distribution of diagnosis with respect to gender

Table 4.30: Mean signal intensity (CSF) for per-contrast and post-contrast with respect to interaction of (TR and TE):

TR	TE		PRE-C	POST-C
190	**4.1**	Mean	245	265
		N	7	7
		Std. Deviation	52.4706	66.036
		Std. Error Mean	19.832	24.959
	4.2	Mean	255	262.5
		N	1	1
	5	Mean	233	225.5
		N	1	1
	5.1	Mean	234.5	249
		N	1	1
520	**11**	Mean	184	219
		N	1	1
	12	Mean	183.769	186.67
		N	52	52
		Std. Deviation	19.2391	22.688
		Std. Error Mean	2.668	3.1463

Table 4.31: Paired Samples t-test for Equality of Means signal intensity (CSF) of pre-contrast and post-contrast with respect to interaction of (TR and TE):

TR	TE		Paired Differences					
			Mean	Std. Deviation	Std. Error Mean	t	df	Sig. (2-tailed)
190	4.1	Pre-C – Post-C	-2.0000	40.3598	15.2546	-1.311	6	.238
520	12	Pre-C – Post-C	-2.9102	9.5155	1.3196	-2.205	51	.032

Table 4.32: Mean signal intensity (white matter) for per-contrast and post-contrast with respect to interaction of (TR and TE):

TR	TE		Pre-C	Post-C
190	**4.1**	Mean	481.42	491.35
		N	7	7
		Std. Deviation	45.073	42.659
		Std. Error Mean	17.0362	16.123
	4.2	Mean	507	537.5
		N	1	1
	5	Mean	448	450
		N	1	1
	5.1	Mean	493	517
		N	1	1
520	**11**	Mean	406	457
		N	1	1
	12	Mean	429.10	444.07
		N	52	52
		Std. Deviation	37.7979	40.506
		Std. Error Mean	5.2416	5.6173

Table 4.33: Paired Samples t-test for Equality of Means signal intensity (white matter) of pre-contrast and post-contrast with respect to interaction of (TR and TE):

TR	TE		Paired Differences					
			Mean	Std. Deviation	Std. Error Mean	t	df	Sig. (2-tailed)
190	4.1	Pre-C - Post-C	-9.9286	8.2484	3.1176	-3.185	6	.019
520	12	Pre-C - Post-C	-1.4971	17.6641	2.4496	-6.112	51	.000

Table 4.34: Mean signal intensity (gray matte) for per-contrast and post-contrast with respect to interaction of (TR and TE):

TR	TE		Pre-C	Post-C
190	**4.1**	Mean	434.429	451.35
		N	7	7
		Std. Deviation	81.7855	84.571
		Std. Error Mean	30.912	31.96
	4.2	Mean	438.5	440.5
		N	1	1
	5	Mean	400	402.5
		N	1	1
	5.1	Mean	530	567
		N	1	1
520	**11**	Mean	379	395
		N	1	1
	12	Mean	345.77	372.46
		N	52	52
		Std. Deviation	36.7907	39.042
		Std. Error Mean	5.1019	5.4142

Table 4.35: Paired Samples t-test for Equality of Means signal intensity (gray matter) of pre-contrast and post-contrast with respect to interaction of (TR and TE):

TR	TE		Paired Differences					
			Mean	Std. Deviation	Std. Error Mean	t	df	Sig. (2-tailed)
190	4.1	Pre-C - Post-C	-1.6929	8.4530	3.1949	-5.299	6	.002
520	12	Pre-C – C	-2.6689	24.0027	3.3286	-8.018	51	.000

Table 4.36: Mean signal intensity (Lesion) for pre-contrast and post-contrast with respect to interaction of (TR and TE):

TR	TE		Pre-Lesion	Post-Lesion
190	**4.1**	Mean	315.35	419.64
		N	7	7
		Std. Deviation	161.83	265.136
		Std. Error Mean	61.168	100.2121
	4.2	Mean	451	753
		N	1	1
	5	Mean	353	340
		N	1	1
	5.1	Mean	331	335.5
		N	1	1
520	**11**	Mean	540	876
		N	1	1
	12	Mean	345.01	561.16
		N	52	52
		Std. Deviation	204.510	344.508
		Std. Error Mean	28.3605	47.774

Table 4.37: Paired Samples t-test for Equality of Means of signal intensity (Lesion) pre-contrast and post-contrast with respect to interaction of (TR and TE):

TR	TE		Paired Differences					
			Mean	Std. Deviation	Std. Error Mean	t	df	Sig. (2-tailed)
190	4.1	Pre-C – Post-C	-1.0429	134.0509	50.6665	-2.058	6	.085
520	12	Pre-C – Post-C	-2.1616	214.9853	29.8131	-7.250	51	.000

Table 4.38: Mean signal intensity of Lesion for pre-contrast and post-contrast with respect to diagnosis:

Paired Samples Statistics				
Diagnose		Mean	Std. Deviation	Std. Error Mean
Tumor	Pre-CE	409.050	150.4978	23.7958
	Post-CE	713.940	256.6324	40.5771
Brain infection	Pre-CE	337.000	81.2312	36.3277
	Post-CE	392.900	141.6715	63.3574
Normal	Pre-CE	0.000	0.0000	0.0000
	Post-CE	0.000	0.0000	0.0000
Atrophy	Pre-CE	395.500	.	.
	Post-CE	457.500	.	.
Benign	Pre-CE	375.611	196.3872	65.4624
	Post-CE	382.556	196.7369	65.5790

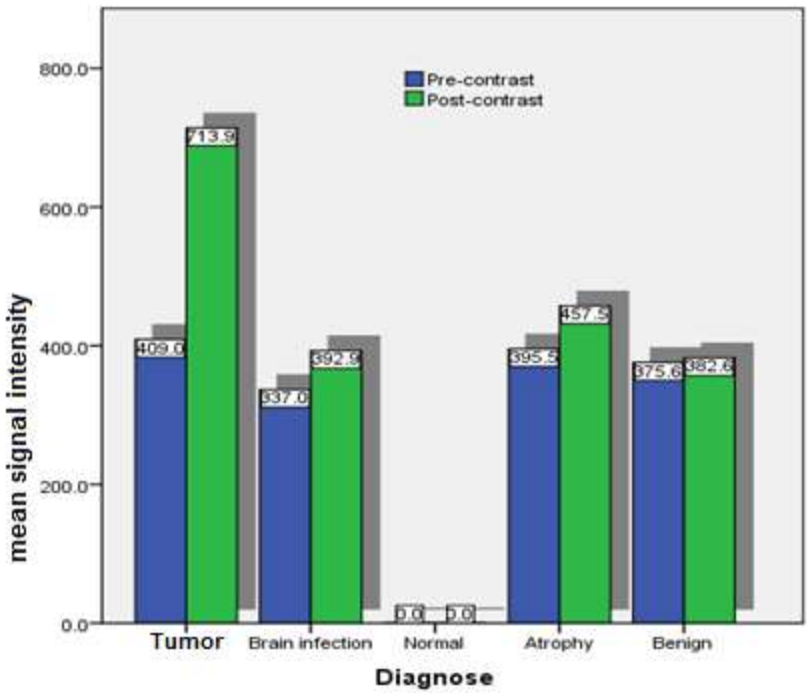

Figure 4.18: Mean signal intensity of type of Lesion for pre-contrast and post-contrast

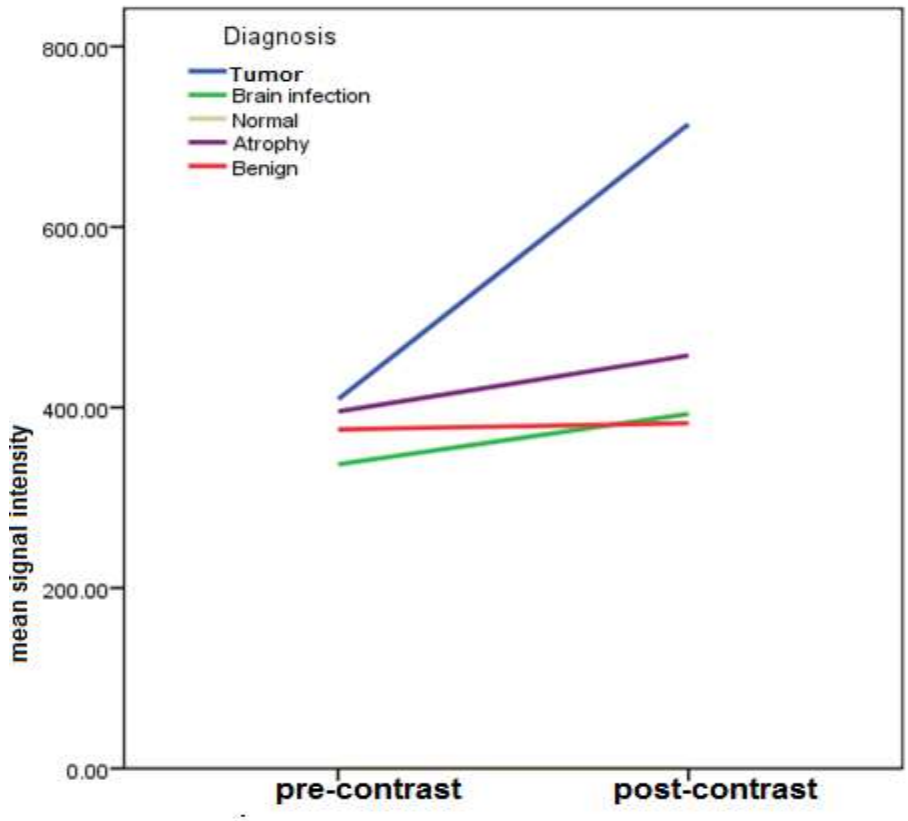

Figure 4.19: Type of Lesion- signal intensity pre- post-contrast

Table 4.39: Paired Samples t-test for Equality of Means signal intensity (Lesion) of pre-contrast and post-contrast:

Diagnose		Paired Differences					
		Mean	Std. Deviation	Std. Error Mean	T	df	Sig. (2-tailed)
Tumor	Pre-CE - Post-CE	-304.89	189.8018	30.0103	-10.159	39	0.000
Brain infection	Pre-CE - Post-CE	-55.900	87.8980	39.3092	-1.422	4	0.228
Benign	Pre-CE - Post-CE	-6.9444	10.7047	3.5682	-1.946	8	0.088

Chapter five

Chapter 5

Discussion, Conclusion, Recommendations

5-1. Discussion:-

The distribution of participants with respect to age show that (9.7%) of participants were less than 10 years old, since (14.3%) of them 10-20 years, (17.5%) of them 2-30 years, (11.1%) of them 31-40 years (14.3%) of them 41-50 years, while (15.9%) of them 51-60 years and (19%) of them were more than 60 years old. . Table (4.1)

The preliminary investigations obtained from this study revealed that the brain lesion patient's participated in this study, distribution with respect to gender (49.2%) of participants were males, while (50.8% of them were females. Table (4.2)

We can see that the mean of (CSF) for pre-contrast and post-contrast are significantly different because the probability value "Sig= 0.013" is less than 0.05. Looking at the means' table (4.3), the researcher concludes that contrast significantly effect on (CSF).

We can see that the mean Signal Intensity of (white matter) for pre-contrast and post-contrast are significantly different "Sig = 0.000" (Sig<0.05). Table (4.5) we can conclude that contrast significantly effect on (white matter).

Also the result indicate that the mean Signal Intensity of (gray matter) are significantly different because the probability value "Sig = 0.000" (Sig<0.05). Table (4.7), we can conclude that contrast significantly effect on (gray matter).

We can see that the mean signal intensity for (Lesion) for pre-contrast and post-contrast are significantly different because the probability value "Sig = 0.000"(Sig<0.05) Table (4.9), we can conclude that contrast significantly effect on (Lesion).

We can see that all of paired means of (CSF) are insignificantly different, (Sig> 0.05).table (4.11), we can conclude that contrast does not effect on (CSF) if age is considered.

We can see that all of paired means Signal Intensity of (white matter) are significantly different, (Sig<0.05), except for more than 60 years. Table (4.13), we can conclude that contrast effect on (white matter) for less than 60 years

We can see that all of paired means Signal Intensity of (gray matter) are significantly different, (Sig< 0.05), except (gray matter) for 51-60 years table (4.15) , we can conclude that contrast effect on (gray matter) for only 51-60 years

We can see that all of paired means Signal Intensity of (Lesion) are significantly different; the values in the (Sig< 0.05), except for less than 10 years and 31-40 years. table (4.17) , we can conclude that contrast effect on (Lesion) is the same for all ages.

We can see that means Signal Intensity of (CSF) are not different for male, the values in the "Sig= 0.197" is more than 0.05, since they are significantly different for female, the values in the "Sig= 0.019" (Sig< 0.05).table (4.19), we can conclude that contrast does not effect on (CSF) for males.

We can see that all of paired means Signal Intensity of (white matter) are significantly different, the values in the (Sig< 0.05) table (4.21), we can conclude that contrast effect on (white matter) for both males and females.

We can see that all of paired means Signal Intensity of (gray matter) are significantly different, the values in the (Sig> 0.05) table (4.23), we can conclude that contrast effect on (gray matter) for both males and females.

We can see that all of paired means Signal Intensity of (Lesion) are significantly different, the values in the (Sig< 0.05).table (4.25), we can conclude that contrast effect on (Lesion) for both males and females.

Notes from the table (4.27), that the most of diagnoses was malignant for all age categories. The probability of the chi-square test statistic (chi-square =12.827) was (Sig. = 0.802), (Sig> 0.05), Thus hypothesis that differences in “diagnosis” are related to age is not supported and diagnosis doesn’t dependent on age.

Notes from the table (4.29), that the most of diagnoses was malignant tumors for both males and females. The probability of the chi-square test statistic (chi-square =3.495) was (Sig. = 0.321(Sig> 0.05) Thus hypothesis that differences in “diagnosis” are related to gender is not supported and diagnosis doesn’t dependent on gender.

We can see that paired means Signal Intensity of (CSF) are insignificantly different for TR,TE: (190 and 4.1) interaction of TR and TE, the value in the "Sig = 0.238" (Sig> 0.05), while paired means of (CSF) are significantly different for TR,TE: (520 and 12) interaction of TR and TE, the value in "Sig = 0.032" (Sig< 0.05). (Table 4.31)

We can see that paired means Signal Intensity of (white matter) are significantly different for (190 and 4.1) interaction of TR and TE, the values in the "Sig = 0.000" (Sig< 0.05), also paired means of signal intensity (white matter) is significantly different for (520 and 12) interaction of TR and TE, the values in the "Sig = 0.000" (Sig< 0.05). Table (4.33)

We can see that paired means Signal Intensity of (gray matter) are significantly different for (190 and 4.1) interaction of TR and TE, the values in the "Sig = 0.002" (Sig< 0.05) and for (520 and 12) interaction of TR and TE, the values in "Sig = 0.000" (Sig< 0.05). Table (4.35)

We can see that paired means Signal Intensity of (Lesion) are insignificantly different for (190 and 4.1) interaction of TR and TE, the values in the "Sig = 0.085" (Sig> 0.05), while paired means Signal Intensity of (Lesion) are significantly different for (520 and 12) interaction of TR and TE, the values in the "Sig = 0.000" (Sig< 0.05), Table(4.37).

The result of statistical analysis showed The mean tumors signal intensity for pre -contrast is different compared to post-contrast -This study Correspond to (Kurk,etal,1995) and (Cheng, etal, 2012)- but with a high heterogeneity (Standard Deviation=256.63) which implies the verity of contrast effect to tumor types.(Table 4.38) This study Correspond to (Stack,etal,1987)

We can see that the mean signal intensity of (Lesion) for pre-contrast and post-contrast are significantly different for diagnosis that (malignant tumors) because its probability value "Sig = 0.000" (Sig< 0.05), while there is no significantly different for (Brain infection and benign)

diagnosis, the probability values "Sig = (0.228 and 0.088)" respectively are greater than 0.05.(table 4.39).

While subject contrast is defined as the difference in some aspect of the signal, the magnitude of the difference in the resultant image can often be affected or adjusted by changing various parameters as the intensity of CSF was affected by the tumor. The increase or decrease of the measure tissue on plane of the slice resulting from the patient movement after the contrast affect the measurement of signal intensity.

5-2. conclusion:

In conclusion, this study has showed that, contrast significantly effect on (CSF, white matter, gray matter, Lesion) but does not effect on (CSF) if age is considered, and the results show that contrast effect on (white matter) for less than 60 years, also effect on (gray matter) for only 51-60 years. While Contrast effect on Brain Lesion is the same for all ages and for both males and females. Contrast does not effect on (CSF) for males that we compared with respect to gender. Contrast effect on (white matter) for both males and females. The diagnosis doesn't dependent on age or gender. There were statistically significant differences in mean intensity change between tissues, with the largest increase for tumor tissue and the verity of the different effect of contrast on tumor types. The results show the ability of contrast agent to identify improve differentiation of tumor detection further establishes contrast agent as a viable tool for detection Brain lesion.

5-3. Recommendations:

The researcher face some problems like: the researcher obtain 83 sample , 20 of these samples was rejected due to deficiencies in the images, the MRI machine in some hospital is not working because the cooling system of the machine is not working ,the computer system of the MRI in some hospital do not respond when using CDs, the computer system of the MRI in some hospital do not accept CDs.

The researcher recommends the follower to perform clinical tests beside the signal intensity measurements for CSF.

Future studies must used large sample to support the findings.

Volumetric signal intensity measurement for lesion may give more information than one position measurement.

Also to obtain a good MRI image the researcher advice the radiographers to avoid the common causes of the patient motion.

The common causes of the patient motion in brain examination are: phobia ,unconscious patients, pain, long scan time, cooling condition in examination room.

Necessarily of QC and Combination with protective maintenance and presence of medical physicist in MRI unit.

References:

Dr_Victor R. Lazar PhD-SRM UNIVERSITY- Magnetic Resonance imaging (MRI) and Magnetic Resonance Spectroscopy (MRS)-MRI Instrumentation 2Aug2012_Part1.

Hitachi Medical Systems America, Inc -MRI Anatomy and Positioning Series | Module 7: Neuro Imaging)

Jerrold T. Bushberg,J. Anthony Seiberg, Edwin M. Leidholdt, Jr.,John M. Boone, The Essential Physics For Medical Imaging, 2nd Ed. 2002 By Lippincott Williams And Wilkins, Philadelphia,USA

Josh Van Den Bossche- MRI "ALL-IN-ONE "Registry Review
B.S., R.T. (R)(MR)- Copyright © 2014.

Jerry Allison Ph.D.Chris Wright B.S.Tom Lavin B.S.Nathan Yanasak Ph.D.
Tom Hu Ph.D. MBA-MRI Contrast Agents-December 12th, 2007.

J. P. Stack,N. M. Antoun,J. P. R. Jenkins,R. Metcalfe,I. Isherwood,- Gadolinium-DTPA as a contrast agent in magnetic resonance imaging of the brain-Neuroradiology-April 1988.

(Laurie Owens BSRT (MR)-20091Patient Preparation and Managementfor MRI Clinical ExamsClarian Health 2009)

Luis Curvo-Semedo and Filipe Caseiro-Alves ,MR Contrast Agents, Verlag Berlin Heidelberg 2011

(Mortamet B, Bernstein MA, Jack CR Jr, Gunter JL, Ward C, Britson PJ, Meuli R, Thiran JP, Krueger G; Alzheimer's Disease Neuroimaging Initiative). -(Magn Reson Med. 2009 Aug;62(2):365-72. doi: 10.1002/mrm.21992.)

Ontario Health Technology Assessment Series 2003; Vol. 3, No. 7-Patient Monitoring System-for MRI An Evidence Based Analysis

Paul M. Parizel , Luc van den Hauwe , Frank De Belder ,J. Van Goethem , Caroline Venstermans , Rodrigo Salgado ,Maurits Voormolen , and Wim Van Hecke- www.springer.com/978-3-540-74501-3 -Magnetic Resonance Imaging of the Brain - P. Reimer et al. (eds.), Clinical MR Imaging, © Springer-Verlag Berlin Heidelberg 2010

Chuang CC, Lee YT, Chen CM, Hsieh YS, Liu TC, Sun CW- Patient-oriented simulation based on Monte Carlo algorithm by using MRI data - Biomed Eng Online (2012)

RadiologyInfo.org -Magnetic Resonance Imaging (MRI) - Body

Timo Kurki, Markku Komu-Spin-lattice relaxation and magnetization transfer in intracranial tumors in vivo: Effects of Gd-DTPA on relaxation parameters-PLUMX-Magnetic Resonance Imaging, ISSN: 0730-725X, Vol: 13, Issue: 3, Page: 379-385-Publication Year:1995.

Yves Gossuin, Aline Hocq, Pierre Gillis and Quoc Lam Vuong - Physics of magnetic resonance imaging: from spin to pixel- Journal of Physics D: Applied Physics, Published 13 May 2010 • 2010 IOP Publishing Ltd

Weiren Cheng, Yuan Ping, Yong Zhang, Kai- Magnetic Resonance Imaging (MRI) Contrast Agents for Tumor Diagnosis- Journal of Healthcare Engineering -(Agency for Science, Technology and Research), Singapore Division of Bioengineering, Faculty of Engineering, National University of Singapore, Accepted for publication November 2012.

www.emedicine.medscape.com/article/2105033-overview

www.medlineplus.gov/ency/imagepages/18117.htm,12-7-2017,2:30)

www.slideworld.org- Magnetic Resonance Imaging (MRI) - Lecture12_MRI

www.theydiffer.com/difference-between-mri-with-and-without-contrast/

www.wikipedia.org/wiki/ MRI Contrast Agent#citeref- Jump up^ "MR Contrast Agents". 2014

www.wikipedia.org/wiki/Human_brain

Appendix

Appendix 1-Data Collection Sheet

No	Age	Gender	CSF.pre.C		CSF.post.C		White matter .pre. C		White matter .post. C		Gray matter. pre.C		Gray matter. post.C		Lesion pre.C		Lesion post.C		Diagnosis	TR.pre.C	TE.pre.C	TR.post.C	TE.post.C
			mean	sd	mean	Sd	mean	sd	mean	sd	mean	sd	mean	sd	mean	sd	mean	sd					

Appendix 2- Example for Image

T1-weighted spin echo images of the brain, before (left) and after (right) injection of a contrast agent:-

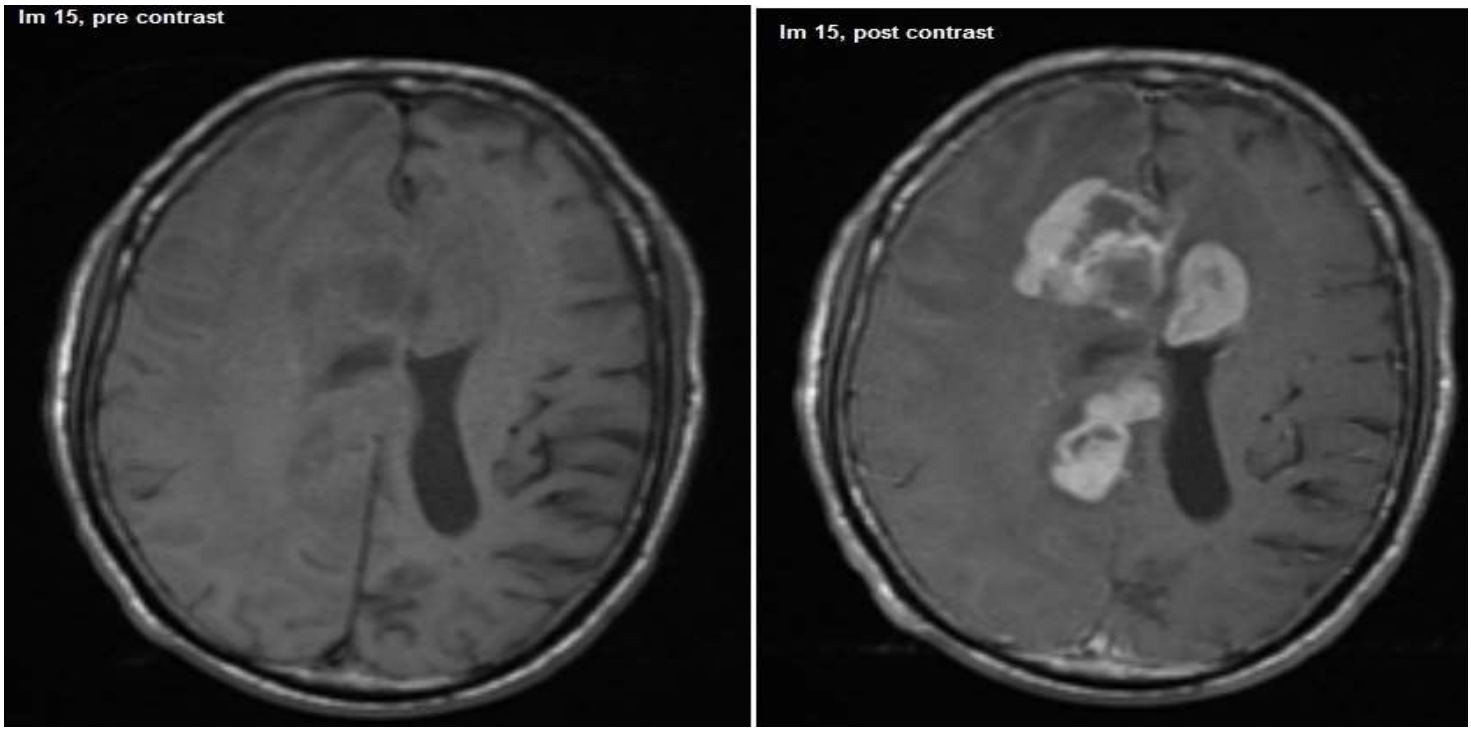

Figure 1: The tumor appears brighter on the right Images - show contrast agent provides additional information for characterization of brain lesion.

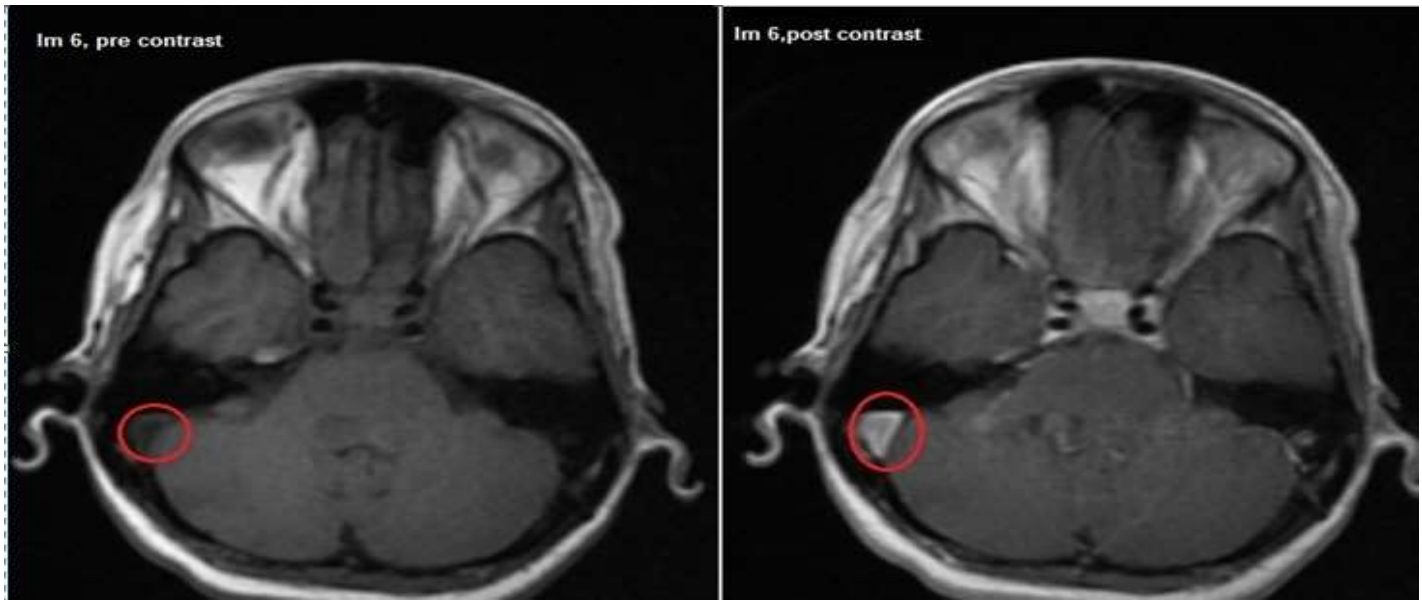

Figure 2: show that in pre-contrast image, the tumor is not clearly defined. The post contrast image, however, shows a clear region of lesion- of 18 years old female

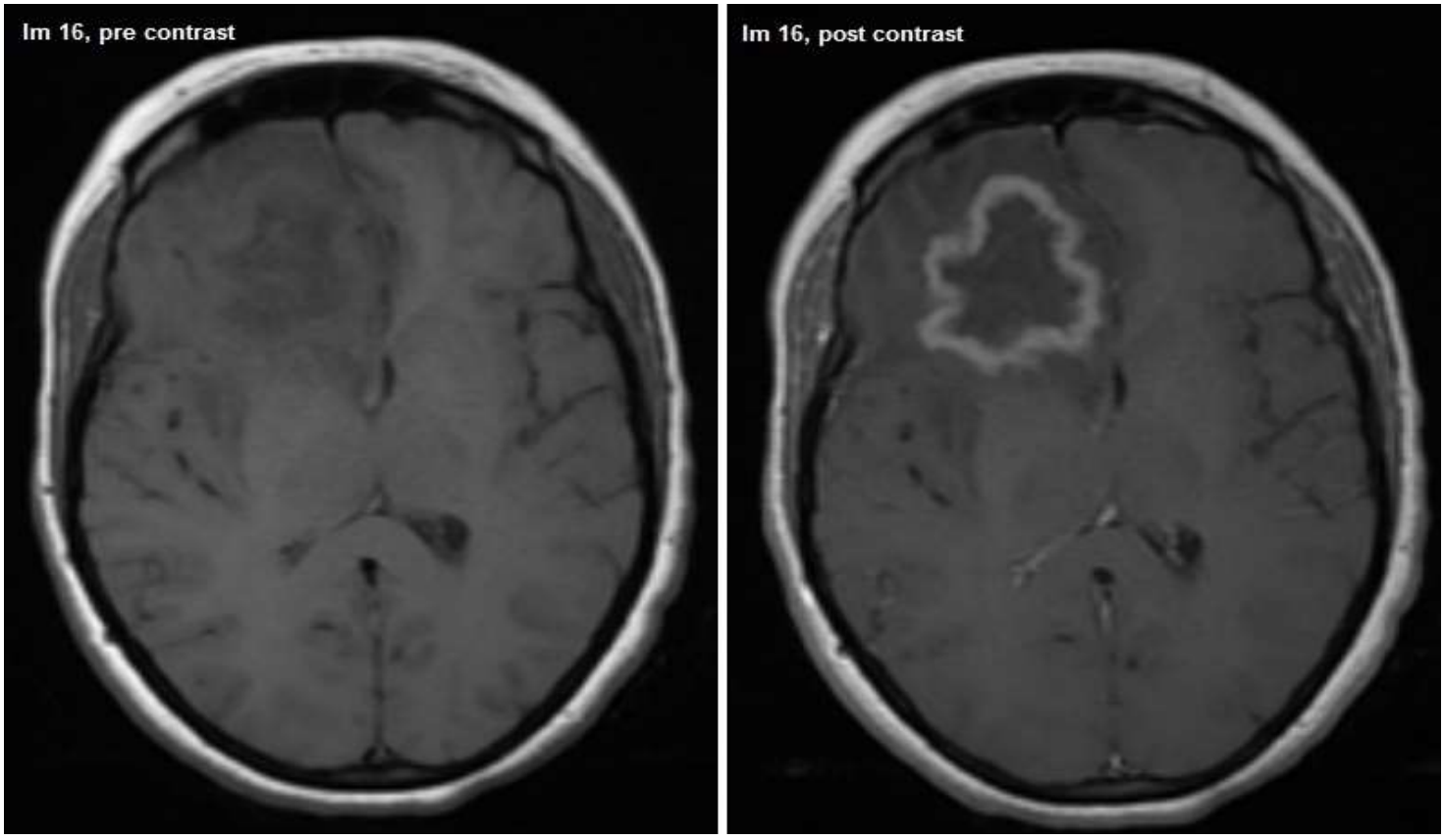

Figure 3: Enhansment in the boundary- of 26 years old female

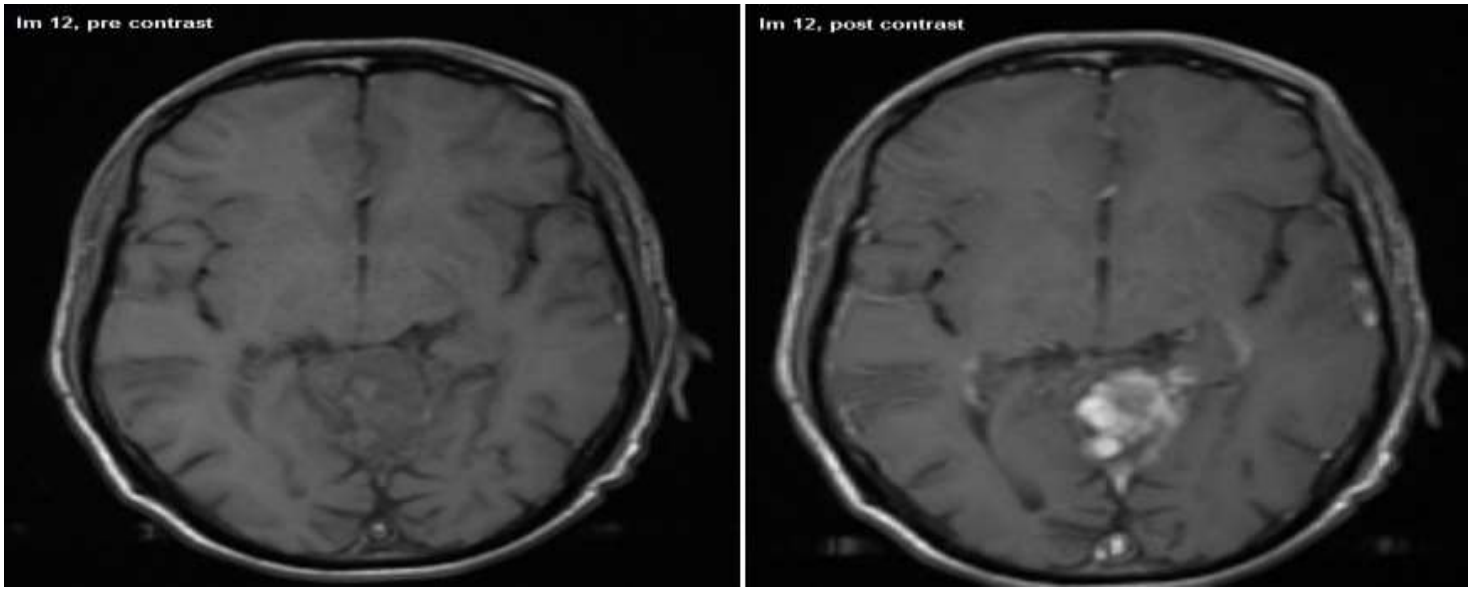

Figure 4: The left image illustrates Brain MRI image void of contrast. The Brain MRI image (right) demonstrates Irregular enhancement- of 45 years old male

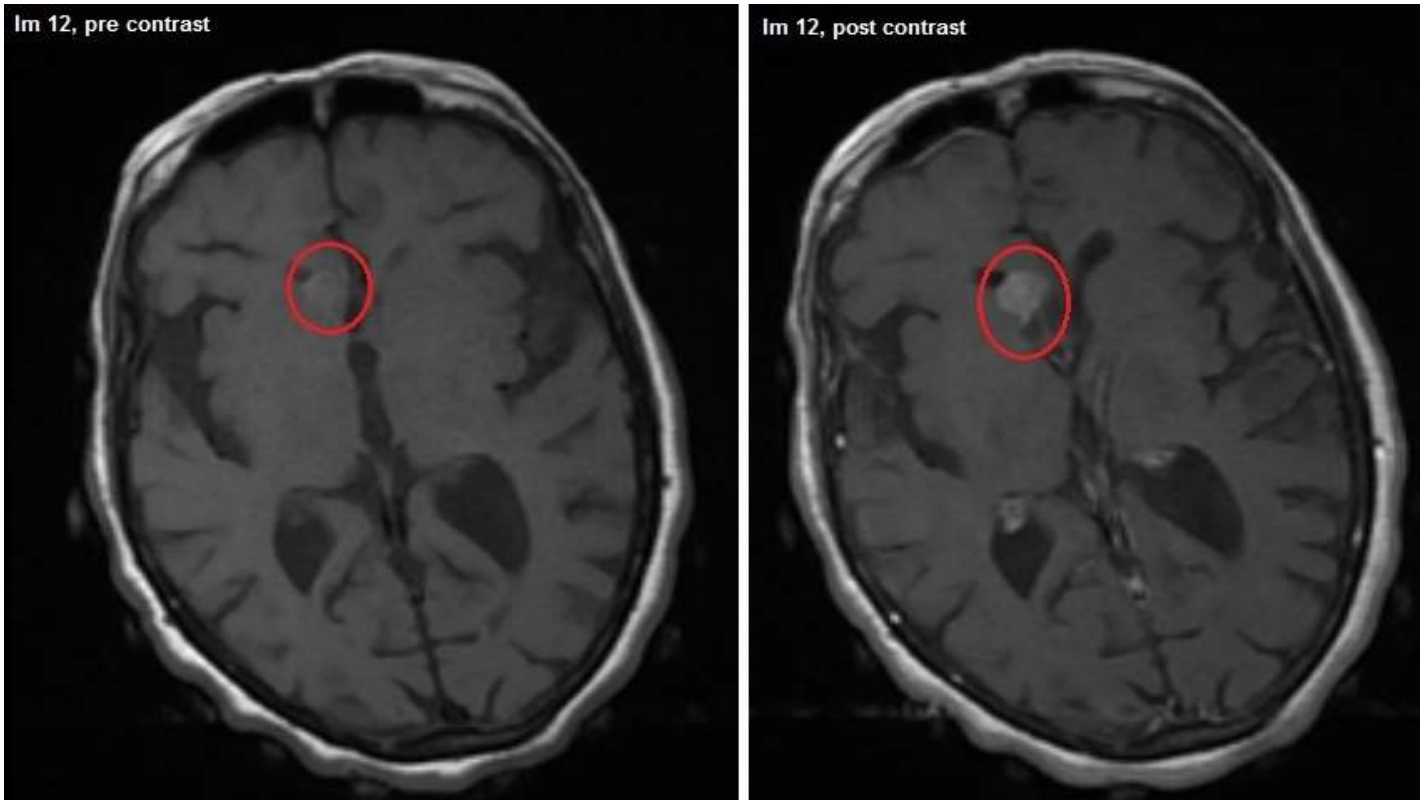

Figure5: In pre-contrast image, the tumor is not clearly defined. The post contrast image, however, shows a clear region of lesion.

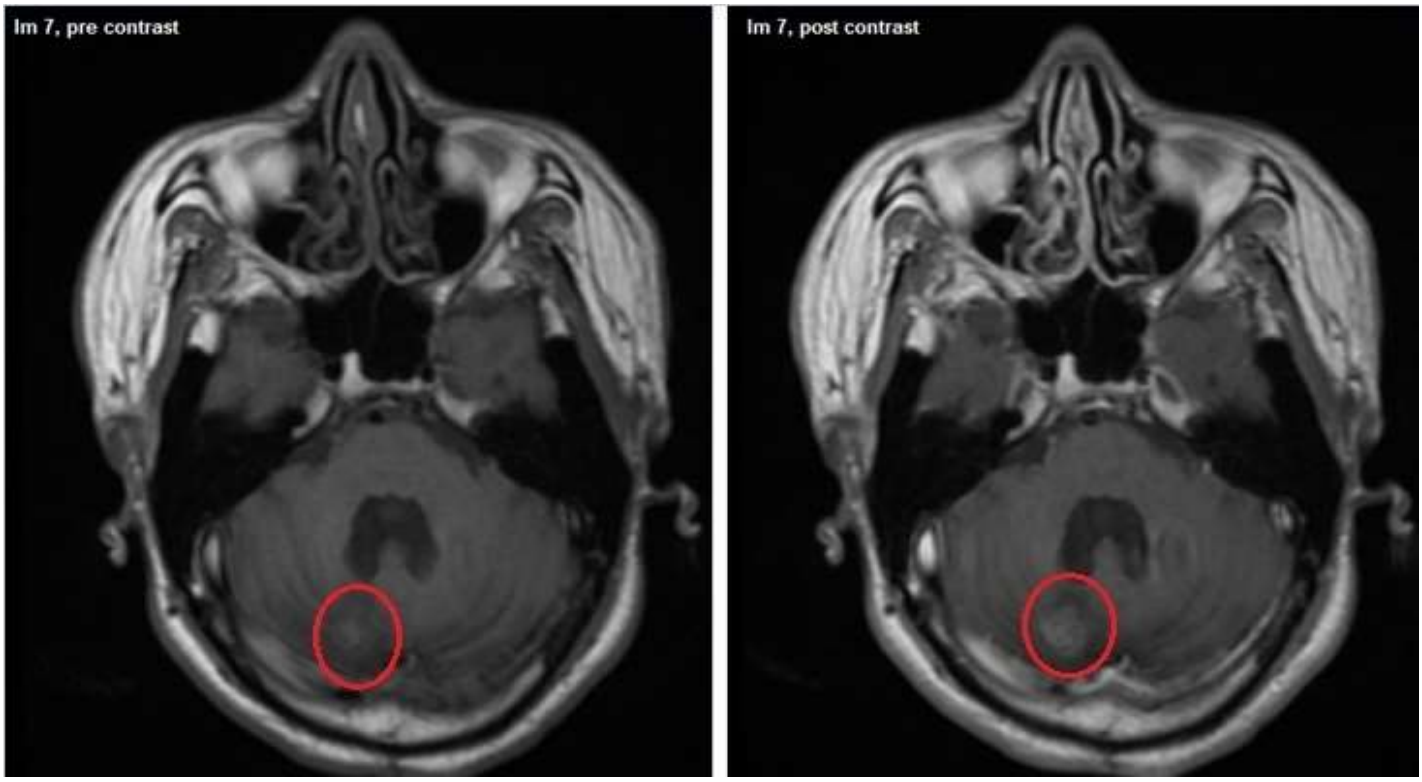

Figure6: The left image illustrates Brain MRI image void of contrast. The Brain MRI image (right) demonstrates a faintly enhancement

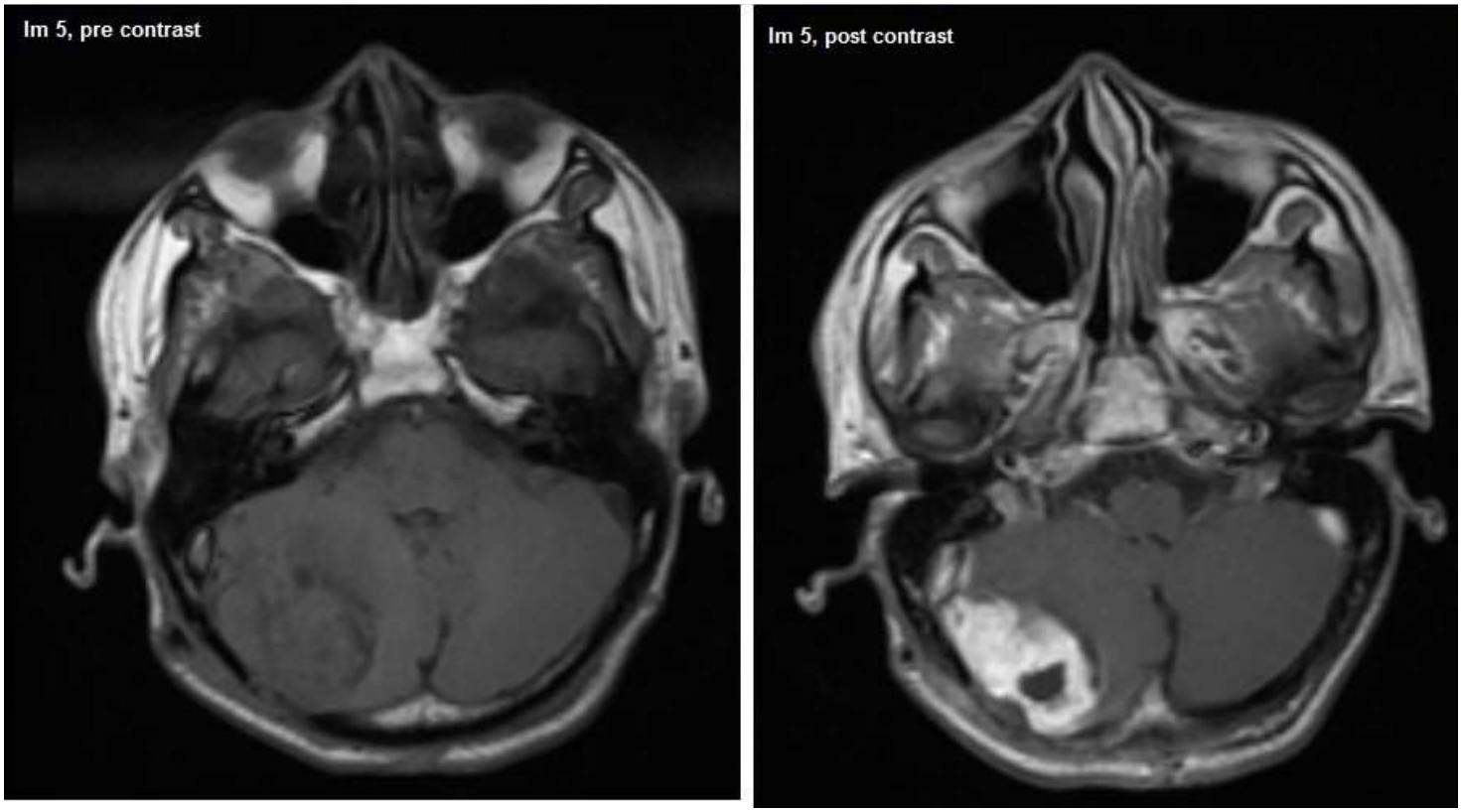

Figure7: MRI image pre and post contrast- Enhancement with Necrotic

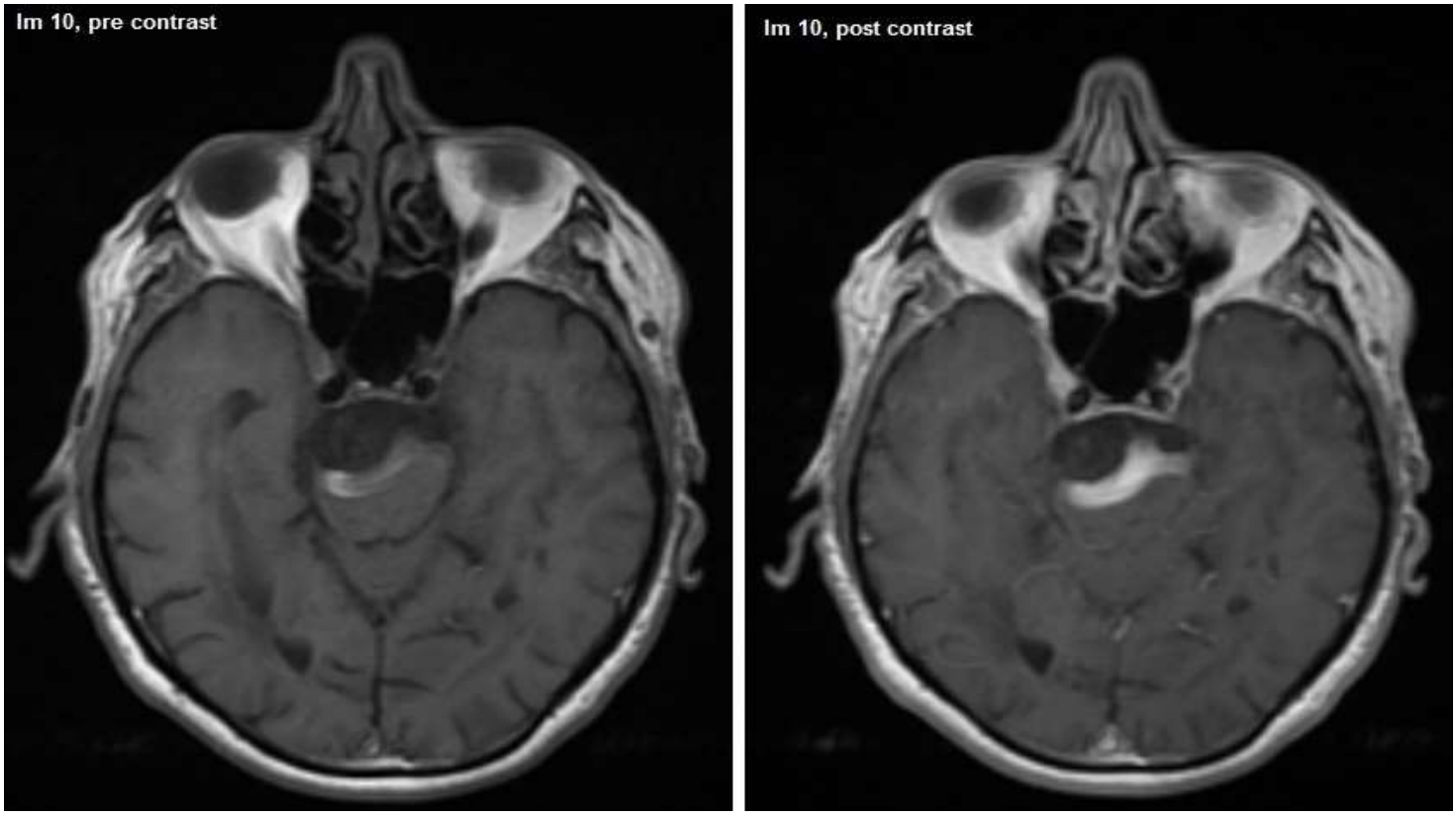

Figure 8: MRI image pre and post contrast -show Mix enhancement

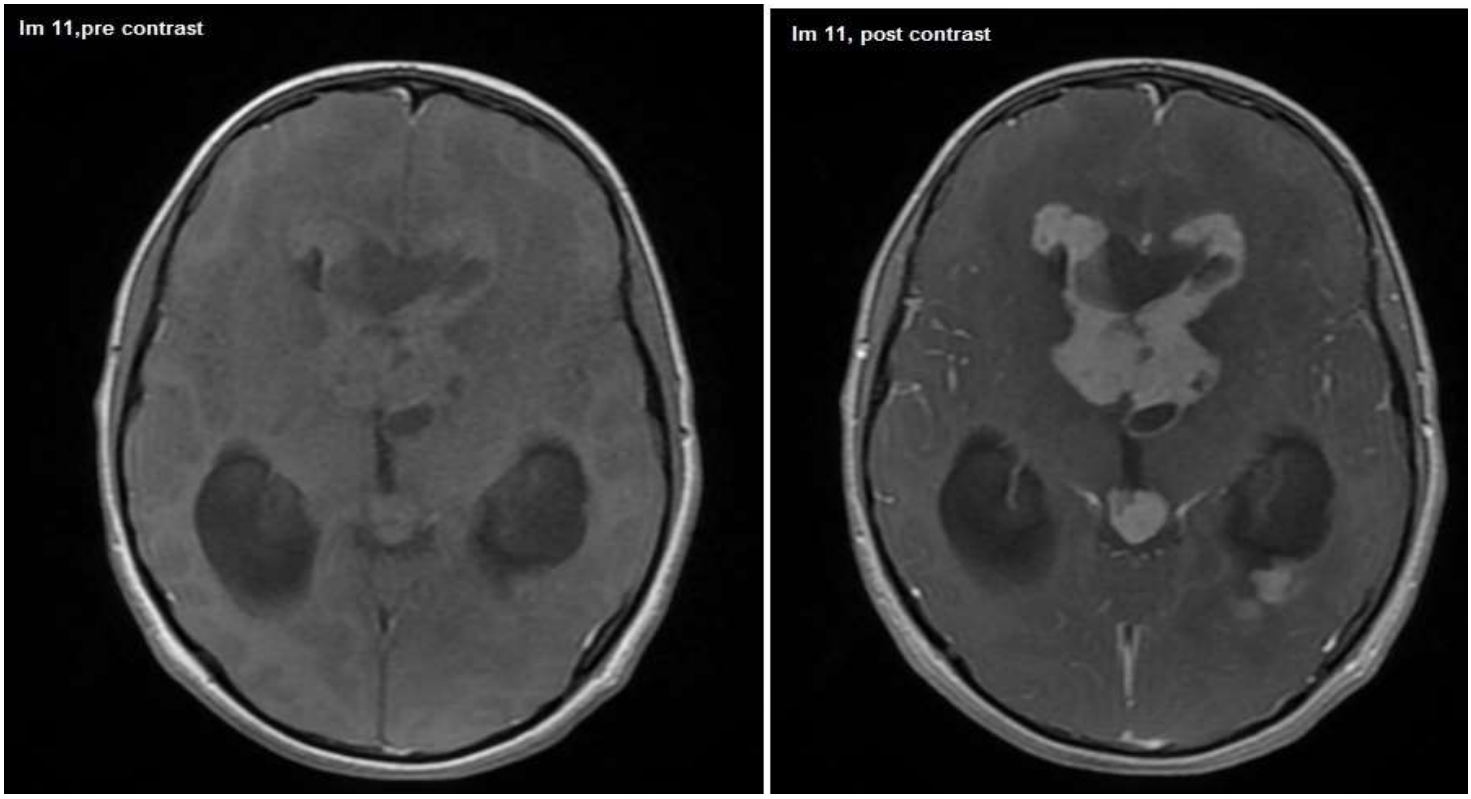

Figure 9: MRI image pre and post contrast-Greater enhancement

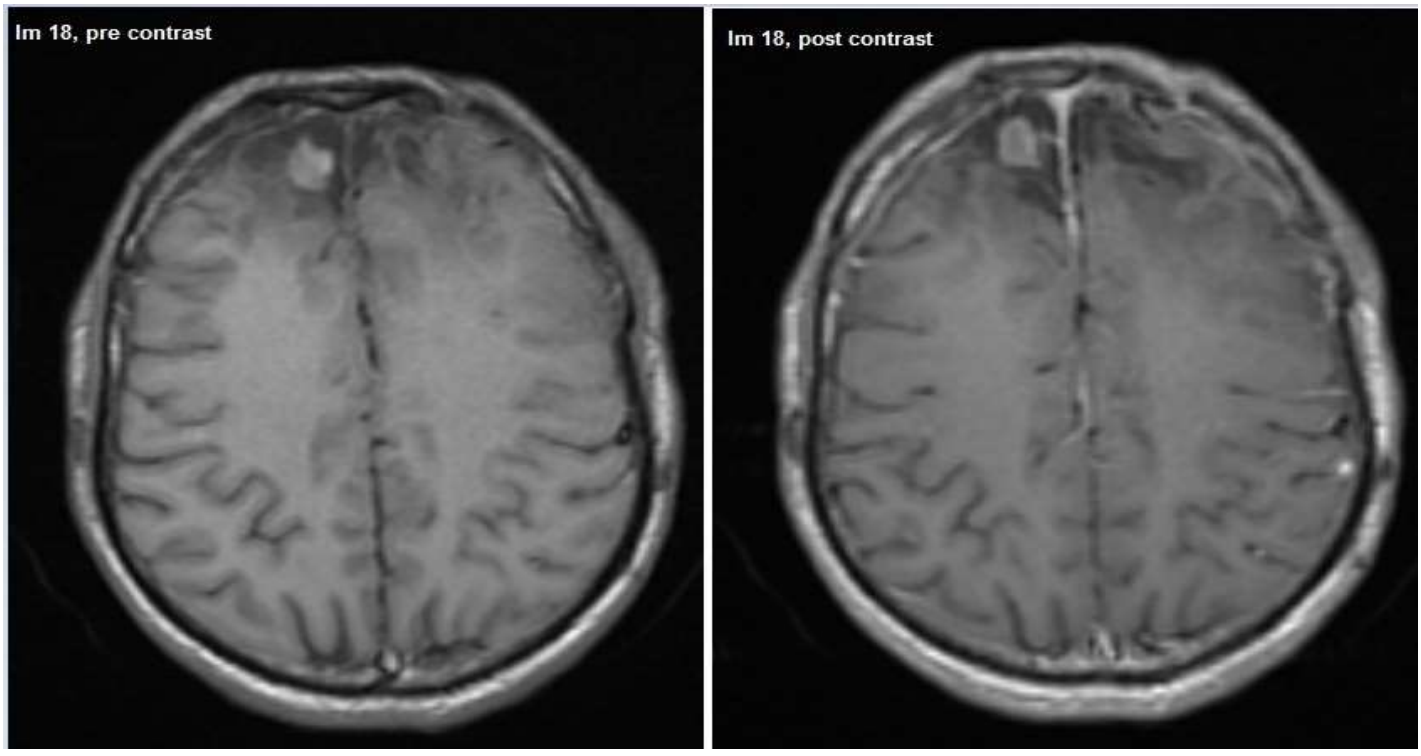

Figure 10: The left image illustrates Brain MRI image void of contrast. The Brain MRI image (right) demonstrates a residual enhancement- of 24years old male.

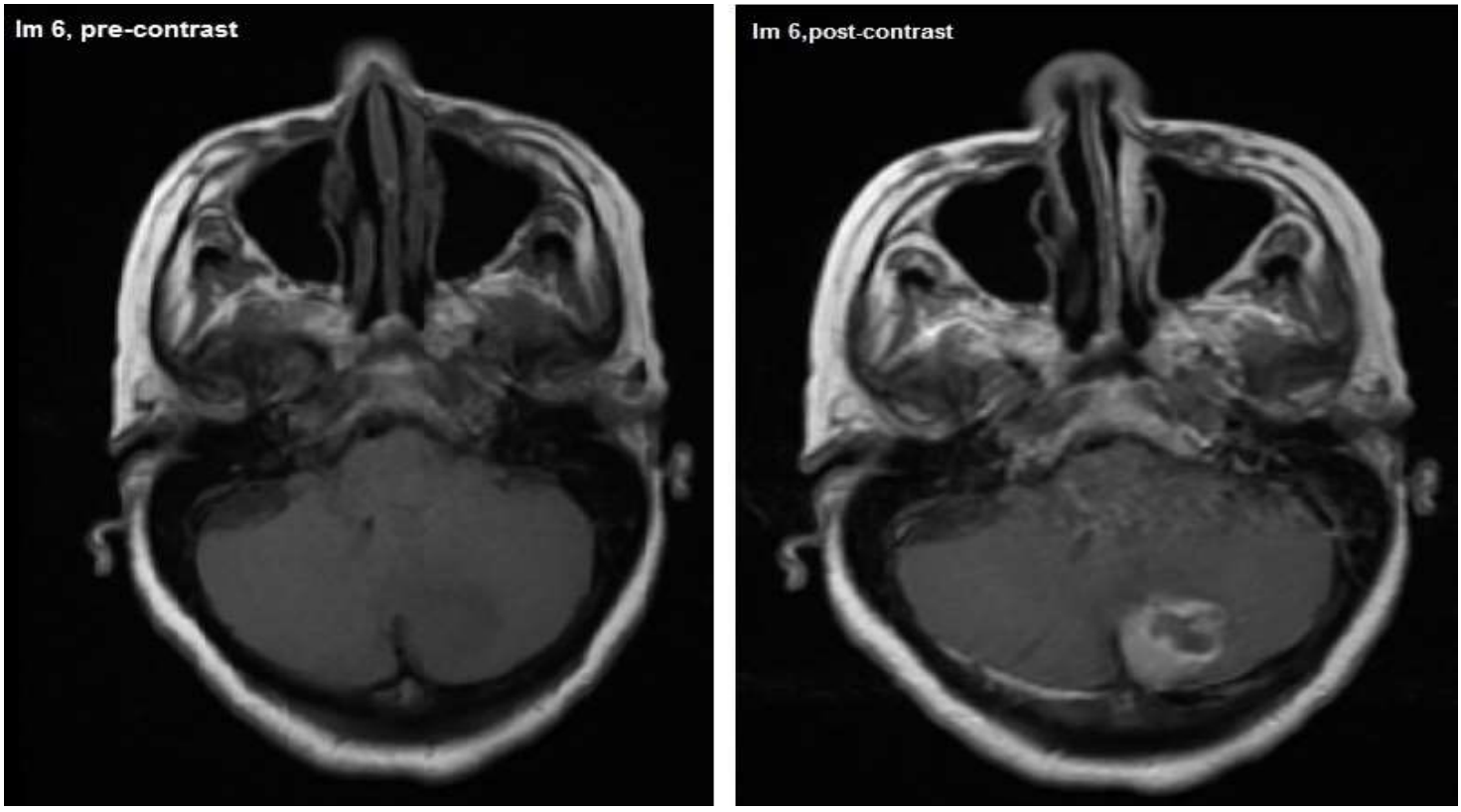

Figure11: MRI image pre and post contrast- Enhancement with Necrotic- of 50 years old female

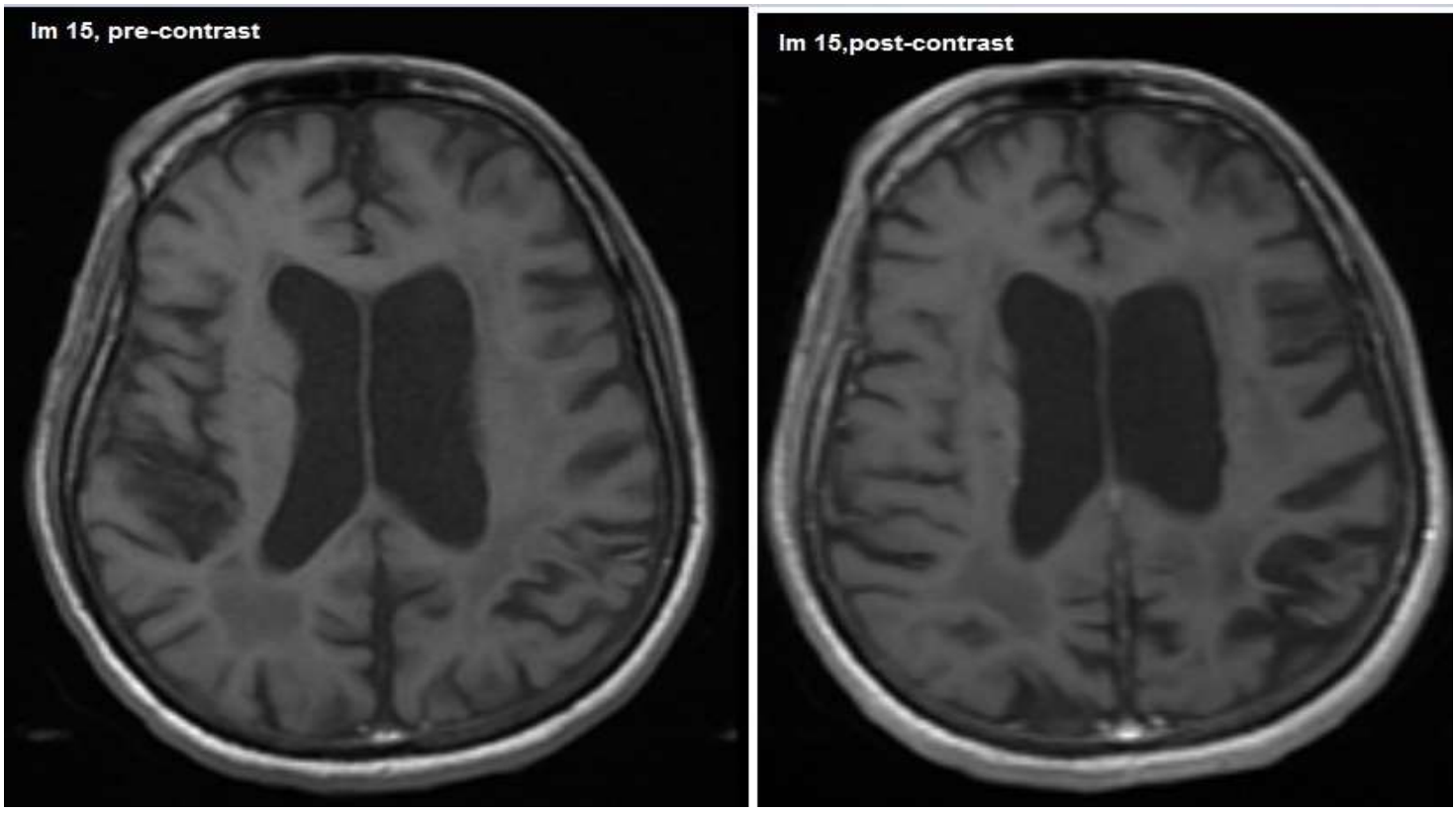

Figure12: MRI image pre and post contrast-Atrophy - of 79years old male

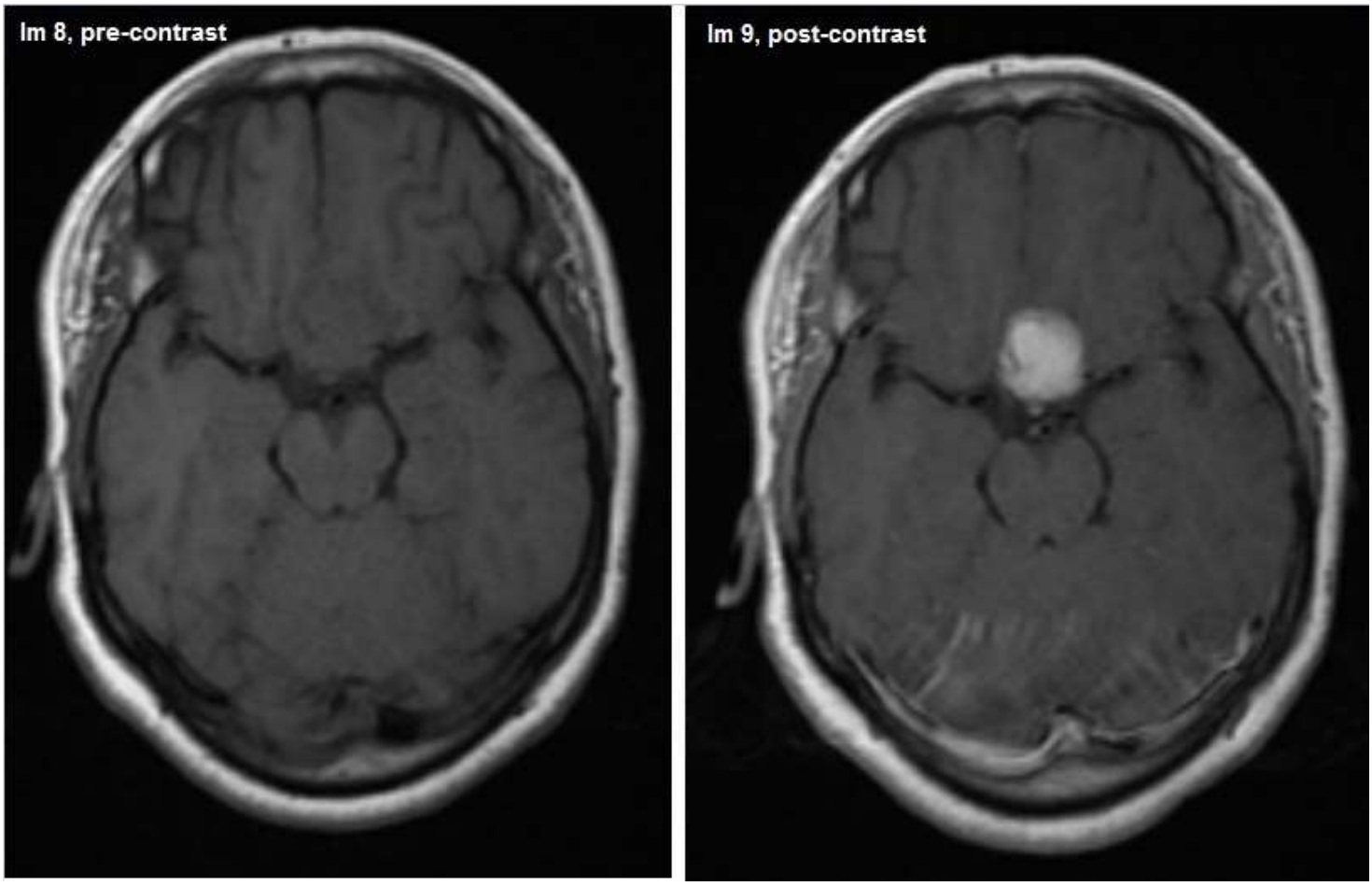

Figure13: MRI image pre and post contrast-Macro Adenoma - of 60years old female